PB-240 568

AIR POLLUTION - ASSESSMENT OF AIR QUALITY IN OSLO, NORWAY. APPENDIX D

K. E. Gronskei, et al

NATO Committee on the Challenges of Modern Society

Prepared for:

Norsk Institutt for Luftforskning, Kjeller

February 1973

DISTRIBUTED BY:

NTIS

National Technical Information Service
U. S. DEPARTMENT OF COMMERCE

085002

COMMITTEE ON THE CHALLENGES OF MODERN SOCIETY

NATO CDSM

OTAN CCMS

PB240568

AIR POLLUTION

Appendix D - Assessment of Air Quality in Oslo, Norway

N.6

POLLUTION ATMOSPHERIQUE

Appendice D - Evaluation de la Qualité de l'Air à Oslo, Norvège

Reproduced by
NATIONAL TECHNICAL
INFORMATION SERVICE
US Department of Commerce
Springfield, VA. 22151

COMITE SUR LES DEFIS DE LA SOCIETE MODERNE

121

BIBLIOGRAPHIC DATA SHEET	1. Report No.	2.	PB 240 568

4. Title and Subtitle
Air Pollution, Appendix D - Assessment of Air Quality in Oslo, Norway,

5. Report Date
February 1973

6.

7. Author(s)

8. Performing Organization Rept. No. 6

9. Performing Organization Name and Address
NATO Committee on the Challenges of Modern Society, 1110 Brussels, Brussels, Belgium.

10. Project/Task/Work Unit No.

11. Contract/Grant No.

12. Sponsoring Organization Name and Address
Office of Air and Waste Management, Environmental Protection Agency, Washington, D. C. 20460

13. Type of Report & Period Covered

14.

15. Supplementary Notes

16. Abstracts

17. Key Words and Document Analysis. 17a. Descriptors
air pollution
air quality
Oslo, Norway

17b. Identifiers/Open-Ended Terms

17c. COSATI Field/Group

Reproduced by
NATIONAL TECHNICAL INFORMATION SERVICE
US Department of Commerce
Springfield, VA. 22151

PRICES SUBJECT TO CHANGE

18. Availability Statement	19. Security Class (This Report)	21. No. of Pages
Available from NTIS	UNCLASSIFIED	121
I	20. Security Class (This Page) UNCLASSIFIED	22. Price 5.25 / MF 2.25

NILU
Intern rapport nr 50/73
IO-00769
Date: February 1973

ASSESSMENT OF AIR QUALITY IN OSLO, NORWAY

by

K E Grønskei E Joranger

F Gram

Published as Appendix D to the

NATO/CCMS Air Pollution Document

"Guidelines to Assessment of Air Quality (Revised)

SOx, TSP, CO, HC, NOx and Oxidants"

Norwegian Institute for Air Research

P.B. 15, 2007 KJELLER

Norway

IA

OTHER NATO/CCMS AIR POLLUTION PUBLICATIONS

Technical Report of the Conference on Low Pollution Power Systems Development, N.4

Proceedings of the Second Meeting of the Expert Panel on Air Pollution Modeling, N.5

Guidelines to Assessment of Air Quality (Revised) SOx, TSP, CO, HC, NOx, and Oxidants, N.6*

Appendix B - Assessment of Air Quality in St. Louis, Missouri, United States

Air Quality Criteria for Sulfur Oxides, N.7*

Air Quality Criteria for Particulate Matter, N.8*

Proceedings of the Third Meeting of the Expert Panel on Air Pollution Modeling, N.14

Air Quality Criteria for Nitrogen Oxides, N.15*

*Also avaliable in French

These documents may be obtained from the NATO Committee on the Challenges of Modern Society, 1110 Bruxelles, Brussels, Belgium, or from the Air Pollution Technical Information Center, Office of Air and Water Programs, Environmental Protection Agency, Research Triangle Park, North Carolina 27711, U.S.A. (English only).

CONTENTS

		Page
1	INTRODUCTION	1
2	DESCRIPTION OF THE STUDY AREA	4
3	SOURCES AND EMISSIONS	9
	3.1 Introduction	9
	3.2 Source inventory	9
	A. General survey	9
	B. The survey of the SO_2-emission	10
	3.3 Results	11
	A. General survey	11
	B. Emission of SO_2	12
	3.4 Concluding remarks	20
4	AIR QUALITY MONITORING	21
	4.1 Introduction	21
	4.2 Monitoring network	21
	4.3 Results	25
	A. SO_2 and suspended particulates	25
	B. Elements in particulate matters	32
	4.4 Concluding remarks	36

Page

5 METEOROLOGICAL MEASUREMENTS 37

5.1 Introduction 37

5.2 Average Meteorological Conditions 40

A. Wind 40

B. Temperature 42

C. Atmospheric stability 42

5.3 Results - Meteorological data 1970/71 45

A. Wind 45

B. Temperature and thermal stability 47

C. The heat-island 50

D. The mixing height 53

5.4 Results of the case studies 55

A. The synoptic situation 55

B. The temperature field 57

C. The variation in temperature with height . 57

D. The wind field 60

E. The wind variation with height 61

F. A model for the wind field 62

5.5 Concluding remarks 71

6 RELATION BETWEEN SO_2-CONCENTRATIONS AND METEOROLOGICAL CONDITIONS 73

6.1 Introduction 73

6.2 Daily mean values 73

Page

6.3 Monthly mean values 76

6.4 Hourly mean values 80

A. Relation between SO_2-concentrations, wind and stability 80

B. Multiple regression between hourly mean values of SO_2 and temperatures 84

C. Relations between SO_2-concentrations and different combinations of meteorological parameters 87

6.5 The investigation of particulate sulphur as air pollution in Oslo 89

6.6 Concluding remarks 91

THE AIR POLLUTION MODEL FOR OSLO 93

7.1 Introduction 93

7.2 Mathematical description 95

7.3 Results 97

7.4 Concluding remarks 105

CONCLUSION 107

PREFACE

The history of the air pollution investigations in Oslo dates back to 1958, when W. Lindberg (1) started the first measurements of SO_2 and suspended particulates in Oslo. His measurements at 10 monitoring stations were concluded in 1965. Later, in 1968 the oil companies started SO_2 measurements, and then in 1969 the Health Authorities in Oslo initiated their measurements of SO_2. In February 1970 the Norwegian Institute for Air Research (NILU), with economic support from the oil companies, started the present study in Oslo, lasting to March 1971. This report deals mainly with the data from the most extensive measuring period, from December 1970 through February 1971.

The object of this study was to:

1. investigate if the gradual reduction of sulphur in the oil consumed in Oslo in the preceeding years, had resulted in a reduction of the SO_2 pollution.

2. develop a model for atmospheric dispersion of pollutants in Oslo by means of a source inventory, meteorological data and imission measurements.

An invitation to add this report to the CCMS report from similar studies in other cities was considered valuable for comparison of methods and results.

A great part of the NILU-staff has been engaged in the monitoring work, and in the preparation of the report from this project. The research group has consisted of: Einar Joranger (project leader), Knut Grønskei (modeling work), Frederick Gram (source inventory and computer programming) and Odd F Skogvold (correlation study of daily SO_2 concentrations). Director of the institute dr. philos. Brynjulf Ottar undertook the preliminary planning and contributed valuable advice in directing this research.

W. Lindberg has kindly placed at the disposal for the project his imission data from 1959-65. The Health Authorities of Oslo have provided data from their three minitoring stations, and the Norwegian Meteorological Institute has supplied meteorological data. A great part of the meteorological equipment was kindly placed at disposal by the Norwegian Defence Research Establishment. The amount of different elements in the suspended particulates, sampled on filters, has been determined at the Norwegian Institute of Atomic Energy by Dr. E. Steinnes.

Grateful appreciation is extended to the Oil Companies and the Norwegian Petroleum Institute for their assistance in making the SO_2 emission inventory.

The illustrations were made by Per Knoph.

1 INTRODUCTION

The present investigation of the SO_2 pollution in Oslo was planned to provide data for analysis along several lines and this was an opportunity to try out methods that can be used to perform similar investigations in other areas. The data analysis was aimed at elucidating the processes that relate the emission of pollution and the ambient air concentrations. The work was not primarily aimed at forecasting future pollution levels, but to develop a tool for connecting emission and air quality.

Two main lines were planned.

1. Regression analysis of the connection between ambient SO_2 concentrations and meteorological parameters that define the "ventilation" in Oslo.

This part was based on a technique outlined by J. Nordø (2), and applied by O. F. Skogvold on meteorological data and SO_2 data collected by W. Lindberg (3). This analysis showed a close correlation between the daily mean SO_2 concentration and a temperature difference, describing the vertical temperature gradient. Thus, this temperature difference could be considered as a ventilation parameter.

The variations of the coefficients in the regression equation between the SO_2 concentrations and this ventilation parameter give information about the emission conditions. It is believed that this method may be used to obtain information about changes in emission conditions from year to year. The emission of SO_2 has a typical daily variation (low emission during the night, larger emission during the day). This diurnal variation in the emission was used to test interpretation of the regression coefficients. This test required measurements of short term ambient air concentrations of SO_2.

Climatological statistics of the vertical temperature gradient was used to compare monthly and quarterly mean values of the air quality. Periods with similar climatological conditions were defined, in order to compare SO_2 concentrations from different years.

2. Detailed short term variation model based on the continuity equation for SO_2.

The Oslo region has a high frequency of periods with stagnated air during the winter time. A model based on a Gaussian diffusion formula is not likely to work properly with these conditions. H. Reiquam (4) has applied a model based on a numerical solution of the continuity equation to the Oslo area. A similar model has been chosen in this work, which offers the possibility of taking into consideration the complex wind fields observed in Oslo.

In order to investigate the wind field and the connection to the SO_2 concentrations, a fairly extensive network of continuous wind measuring stations was planned. Together wit

the continuous wind measurements half hourly SO_2 measurements were performed. In addition, a number of case studies were made in order to establish in detail the connection between wind, temperature and air pollution concentration. It was planned to use an aircraft together with radiosondes, wiresondes and pilot balloons in order to get an idea of the vertical variations of wind and temperature.

In order to get a continuous registration of the temperature variation with height, a chain of thermographs was placed along the hillside north of the city (see Figure 5.1). The results from the regression analysis (3) gave the idea to this chain of thermographs. The ability of the thermograph measurements to represent the vertical temperature gradient above the centre of the city, was tested by means of wiresonde measurements. A thermograph placed in a small park in the centre of the city made possible continuous observations of the "heat-island"-effect. The temperature measurements from the thermograph chain and from the centre of the city was used in an attempt to define the mixing height.

The emission inventory was performed in cooperation with the oil companies.

The method for daily analysis of SO_2 demanded filtration of the air sample. The filters provided samples for determination of the chemical elements in the suspended particulates.

2 DESCRIPTION OF THE STUDY AREA

Oslo is the administrative centre of Norway. It also has some industry. In Figure 2.1 the Oslo area is shown.

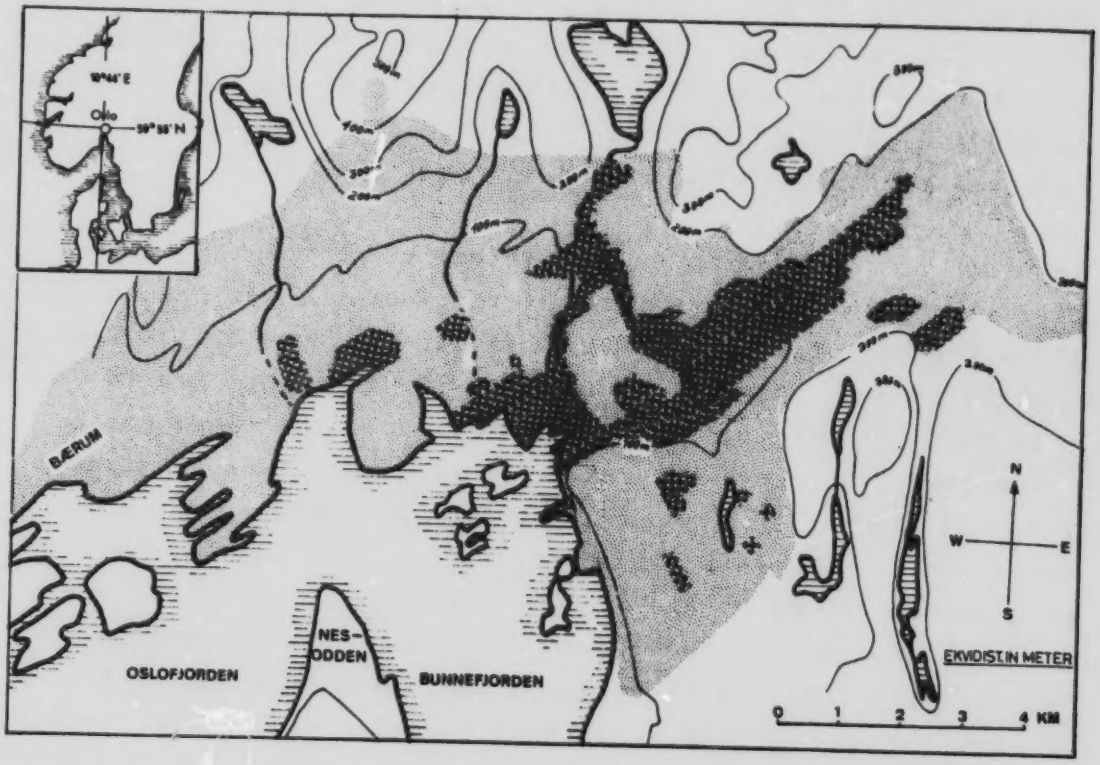

Figure 2.1: Oslo study area.
Residential area.
Industrial area.

The Oslo study area consists of the Oslo, Nesodden and Bærum communities. The population of the study area in 1970 was:

	Inhabitants	Area (km^2)
OSLO	487 363	450
NESODDEN	9 029	60
BÆRUM	74 655	190
Total	570 047	700

Figure 2.2 shows the population density of the area.

Oslo is situated in a basin, at the end of the 100 km long Oslofjord. Within a radius of 6 to 12 km from the city centre, the area is shielded by hills of heights between 200 and 500 meters a.s.l. The long north-south directed main valleys in southern Norway have their outlets east and west of Oslo. The valleys with outlets into the Oslo-basin are short (15-20 km). The main drainages are from the east-northeast (ENE), nortnorthwest (NNW), and south (S) (along the Bunnefjord into the central part of the area).

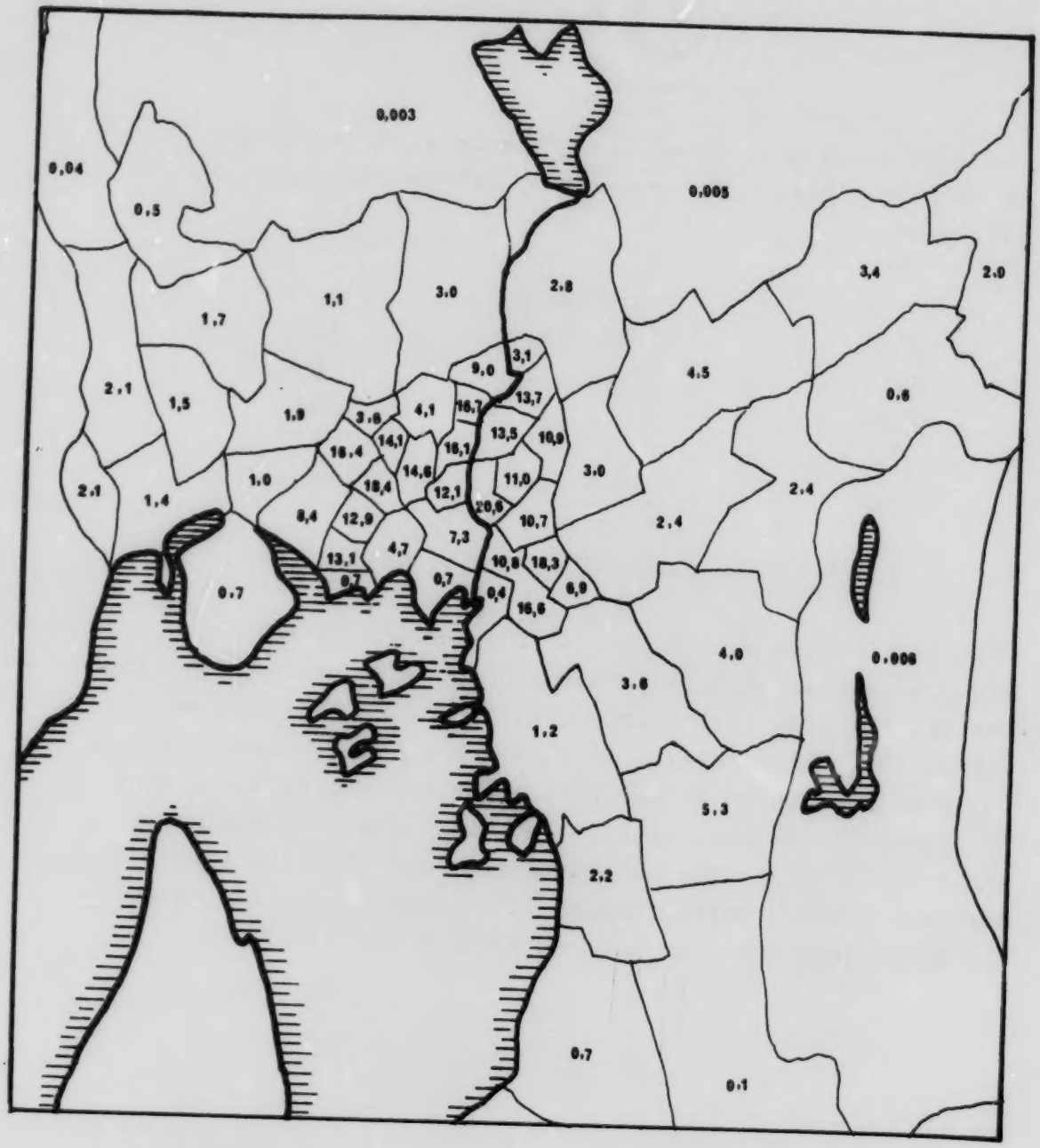

Figure 2.2: Population densities in the Oslo area.
Units: Inhabitants per km^2.

The drainage of cold air along the Oslofjord is restricted by the narrow sound at Drøbak with 200-300 m high ridges on both sides. Figure 2.3 shows a marked basin below the 80 meter-contour line. The climate in Oslo is more continental-like than oceanic because the city lies at the end of a deep fjord. The average monthly temperature of January is -4.7°C and of July 17.3°C. Prevailing winds during the autumn and winter are weak and mainly from the north. During spring and summer, the prevailing winds are stronger and mainly from the south. The pollution level has a maximum during the winter with stagnant air and inversions. In these cases, stable air flows into the basin from northwest, north, east, and south.

Figure 2.3:
The Oslo basin.

Normally, the surface of the water body between the islands in the inner part of the Oslo-fjord is frozen during the winter months. Some winters, ice covers the fjord to the outlet at Drøbak.

In the Oslo area, fuel oil accounts for approximately 60% of the energy consumption for heating. The rest (40%) is supplied by hydroelectric power. The Health Authorities of Oslo have the responsibility for the current control of air pollution. From 1970, limits were set for the content of sulphur in the fuel oil to be used in Oslo. For furnace installations with assumed consumption of less than 700 tons, the sulphur content must be less than 0.8 weight percent. With annual consumption above 700 tons, the sulphur content must be below 2.5 weight percent.

3 SOURCES AND EMISSIONS

3.1 Introduction

Since the object of this investigation was primarily to study the connection between concentrations of SO_2, emissions and weather conditions, collection of emission data was concentrated on the sources of SO_2. However, an estimate of the emission of other pollutants is also given.

In this study, it was necessary to obtain the emission data in a grid system. The UTM-system with 1 x 1 km^2 squares was chosen for this purpose.

3.2 Source inventory

A. General survey

When doing a general emission inventory, the sources of pollution may be classified into the following four categories:

(1) fuel combustion in stationary sources,
(2) fuel combustion in mobile sources,
(3) industrial processes,
(4) solid waste and refuse disposal.

The emission data were collected from different institutions. Data on the sales of fuels, collected by the Health Authorities in Oslo, were used to estimate the emission from stationary sources. Emission from motor vehicles was estimated from the consumption of gasoline in the Oslo area (5).

Quantitative data on the emission from industrial processes has not been available. Regarding the SO_2-emission, the contribution from this category is small. The contribution from refuse disposal is roughly estimated (6).

B. The survey of the SO_2-emission

The SO_2-emission was investigated extensively, in order to give adequate emission data for the model-calculations.

As shown below in Table 3.1, the principal sources of SO_2-pollution in Oslo is combustion of oil in stationary sources. The long term trends of the total SO_2-emissions in Oslo were extracted from official sales statistics for the last 10 years.

The oil companies supplied information about the delivery of sulphur (in oil) to each square kilometer in the Oslo area during the first three months of 1970. This information was the best measure available for the actual emission of SO_2 for the winter 1970.

For the spatial resolution of SO_2-emission in the first three months of 1971, and for the estimate of the time variation of the emission, the oil companies gave information on the following:

a) the total sale of different types of oil and their sulphur content for every three months of 1970, and the first three months of 1971.

b) detailed delivery data for customers with a yearly consumption of either 200 tons of heavy oil or more than 500 m^3 of light oils.

In order to determine the daily, weekly, monthly, and yearly variation in oil consumption and the emission conditions (chimney heights etc), questionnaires were also sent to the largest oil consumers in the region.

3.3 Results

A. General survey

The emissions of the dominant air pollutants in the Oslo area in 1970 are summarized by source in Table 3.1.

SOURCE CATEGORY		Sulphur Oxides as SO_2	Particulates	Carbon Monoxide	Hydro-Carbons	Nitrogen Oxides as NO_2
FUEL COMBUSTION in MOBILE SOURCES	GASOLINE	120	160	68 000	9 800	3 300
	DIESEL	420	420	1 100	2 000	1 200
FUEL COMBUSTION in STATIONARY SOURCES	OIL	8 730	480	n	n	1 180
	COAL & COKE	230	420	n	n	170
REFUSE DISPOSAL	INCINERATION	100	30	n	n	n
INDUSTRIAL PROCESSES		n		n	n	n
TOTAL		9 600		69 100	11 800	5 850

Table 3.1: Air pollutant emissions in Oslo 1970, in metric tons per year.
n = negligible

Industrial processes may contribute significantly to the emission of particulates in Oslo, whereas for the other pollutants tabulated, they may be considered to be of minor importance.

Apart from suspended particles, SO_2 seems to represent one of the highest air pollution stresses on a regional scale, in relation to the ambient air quality standards. On a local scale, however, the pollutants associated with motor vehicles (CO, HC, NO_x) may represent the most serious problem.

Table 3.1 shows that the dominant source of SO_2-emissions in Oslo is the combustion of fossile fuels, mainly oil in stationary sources. In 1968, the SO_2-emissions from the combustion of coal, coke and natural gas were less than 2% of the total SO_2-emissions, and no single consumer of coal, coke or gas emitted more than 20 tons SO_2/year.

Compared to other metropolitan areas of comparable size, Oslo has a low total emission of sulphur. This is partly due to the extensive use of hydroelectric power in both the industrial and domestic sectors.

B. Emission of SO_2

Previous emission trends:

Figure 3.1 shows the emissions of SO_2 for the period 1960-1970. The figures are based on official data for the sale of oil for industrial use and space heating.

The solid lines represent the amount of oil purchased by customers located in Oslo. This oil, however, is not entirely consumed within the Oslo area.

Also included in the figure is data (broken line) representing the SO_2 emissions as estimated by the oil companies. This estimate includes heavy oil only (2.0-2.3% S) and is based on the actual oil delivery addresses. The discrepancy between the two estimates is considerable. However, most of this may be explained by the fact that some of the purchased oil in Oslo is not consumed locally. A study of the 1970 data shows that oil purchased in Oslo corresponding to 4570 tons of SO_2 was consumed outside the city, thus taking care of the shown discrepancy.

Since this division into locally and not locally consumed oil is not known for all the years in the entire period, the curve marked "total" may only represent a rough estimate of the SO_2 emission trend.

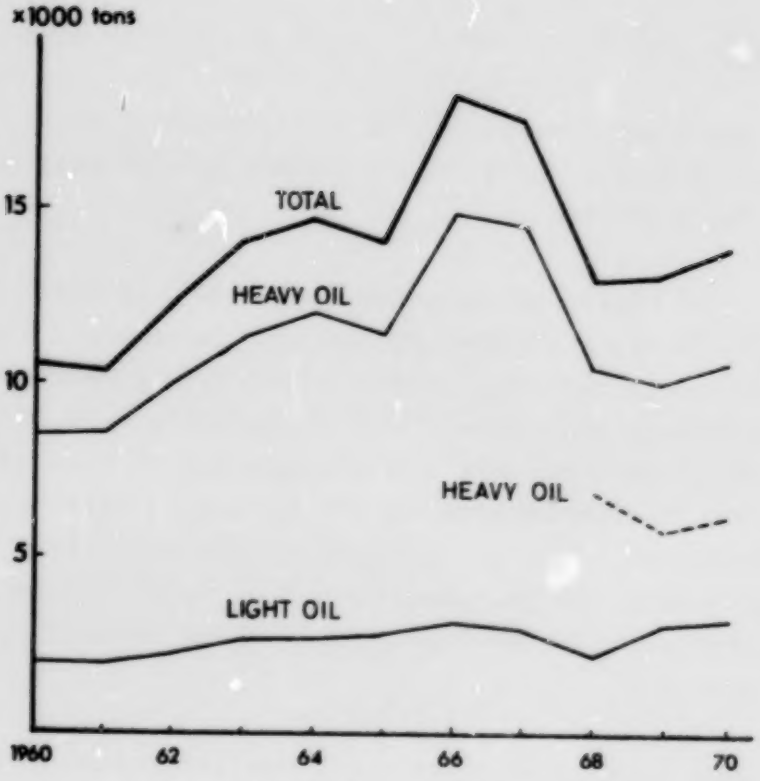

Figure 3.1: SO_2 emission from oil combustion.
——— data based on Oslo invoice addresses
----- data based on Oslo delivery addresses.

Figure 3.1 shows that the SO_2 emissions increased from 1960 to 1966 followed by a decrease (about 30%) for the 1966-1968 period. In comparison the total oil consumption in Oslo increased with approximately 2000 tons per year during the entire period.

Data supplied by the oil companies sometimes show large differences in sulphur content for similar oil qualities. For the period 1968-70 the mean percentages were 0.5 - 0.6% sulphur

for light oils and 2.0 - 2.3% sulphur for heavy oils. Occasionally heavy oils with a sulphur content down to 0.5% was delivered.

The seasonal variation of the SO_2 emissions from oil combustion during 1970 is shown in Table 3.2.

	Light oils	Heavy oils	TOTAL
January-March	1 010	2 630	3 640
April-June	330	1 160	1 490
July-September	320	660	980
October-December	990	1 630	2 620
1970	2 650	6 080	8 730

Table 3.2: 1970 emissions of SO_2 in Oslo from delivery address data, in tons of oil.

The data in Table 3.2 are based on data mainly from the oil companies in the Oslo area. In some cases the data cover a larger area than the city of Oslo. When possible, this has been corrected for, and the data in Table 3.2 may therefore be considered as representative for the SO_2 emissions from oil consumption in Oslo in 1970.

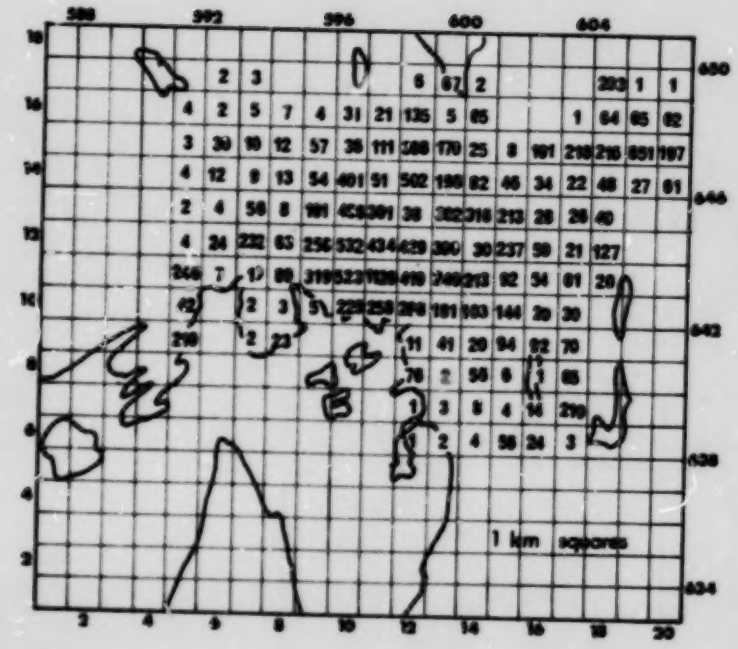

Figure 3.2:
Delivery of sulphur in oil January - March 1970.
Unit: 100 kg S/km².

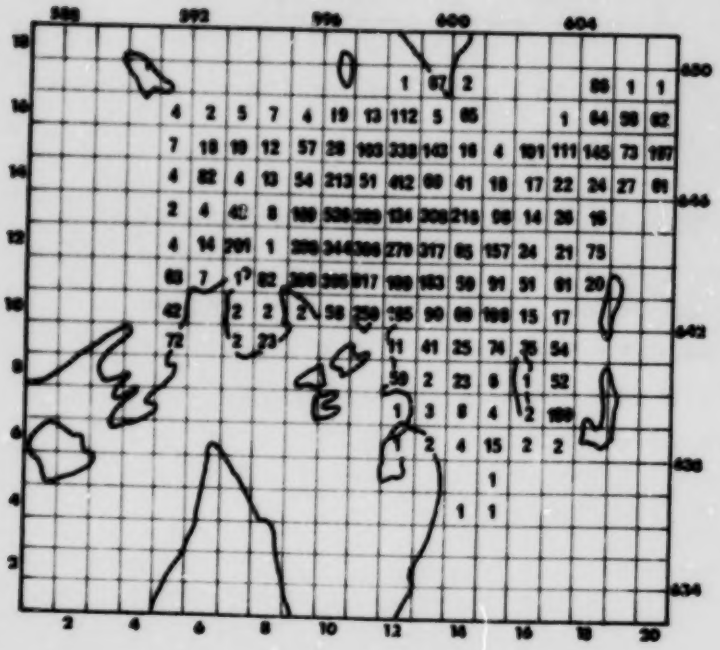

Figure 3.3:
Delivery of sulphur in oil January - March 1971.
Unit: 100 kg S/km².

Area-wise distribution

The data representing the sulphur content in oil delivered within each km^2 of Oslo in the first three months of 1970 and 1971 are presented in Figures 3.2 and 3.3 respectively. The numbers in Figure 3.3 are estimated from the change in the sulphur content of oil delivered, from the winter of 1970 to the winter of 1971, to the 150 largest oil customers. This gives an estimated decrease in the SO_2 emissions of approximately 30 percent.

Figure 3.4 shows the location of the largest sources of SO_2 in Oslo. There are only 8 point sources of SO_2 with emissions exceeding 100 tons/year (1970).

According to the questionnaires the stack heights for the large SO_2 sources are 20-60 m in the central parts, and 30-50 m in the outer regions.

Diurnal and daily variation

A comparison of daily data for the oil consumption at some municipal buildings in Oslo (hospitals, schools, office buildings) in 1969 with the degree-day number for station B (Blindern, see Figure 5.1) showed that the degree-day number may be used to estimate the daily emissions. The degree-day number denotes the deviation of the actual daily mean temperature from $17^{\circ}C$. The daily variation in the consumption of electric power follows a similar pattern, thereby supporting the assumption above.

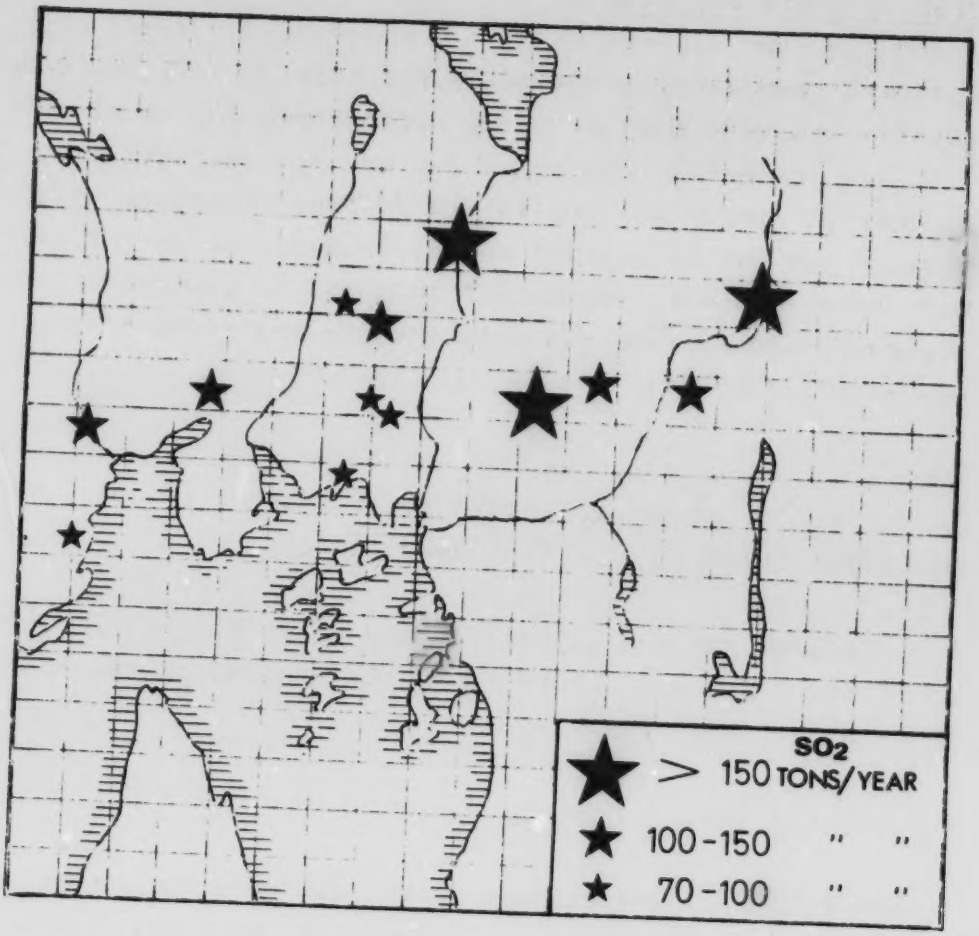

Figure 3.4: Location of the largest sources of SO_2 in Oslo.

From the data supplied by the large oil consumers it was found that the diurnal variation in oil consumption followed different patterns (differences in heat control-systems and combined use of oil and electricity).

As a first approximation for the model calculations, empirical data on the diurnal variation of the oil consumption from USA were used (7). According to these data the hourly emission of SO_2 may be calculated from the seasonal delivery of sulphur in oil according to the following formula:

$$Q_{SO_2}(T_i, t_h) = f(t_h) \cdot \frac{17 - T_i}{\sum_k (17 - T_k)} \cdot Q \qquad \text{(Eq 3.1)}$$

$Q_{SO_2}(T_i, t_h)$: emission of SO_2

T_i : actual daily mean temperature

t_h : hour of the day

$\sum_k (17 - T_k)$: : total of the seasonal degree-day numbers.

Q : seasonal delivery of sulphur in oil, (calculated as SO_2). See Figure 3.2 and 3.3.

$f(t_h)$: hourly fraction of the daily emission (empirical values).

3.4 Concluding remarks

As a conclusion of this survey it may be said that due to the extensive use of electric energy the emission of SO_2 is small in Oslo compared with cities of similar size. The pollution from motor vehicles contribute significantly to the total air pollution stress in the region. Since these pollutants are emitted close to the ground, the most serious pollution problem in Oslo may be found in the areas with heavy traffic.

Large discrepancies are found between data on oil consumption in Oslo when based on invoice addresses respectively delivery addresses, due to the fact that a fraction of the oil purchased in Oslo is actually consumed outside Oslo. The sales-statistics based on invoice addresses show a decrease in the SO_2 emission from 1966 to 1969, but the largest decrease is found from 1967-1968. This is due to a reduction of the sulphur content in the oil. Due to the inconsistencies in the data it is not possible to quantify the reduction of the sulphur emission in the Oslo region for this period.

The data for the oil consumption based on delivery addresses, show a significant reduction in the SO_2 emission (about 30%) from the winter 1970 to the winter 1971. This is partly due to the restrictions that are imposed on the oil consumers in Oslo.

4 AIR QUALITY MONITORING

4.1 Introduction

The first monitoring program for SO_2 pollution in Oslo was operated by Lindberg (1) in the period 1958 to 1965 with a network of 10 stations.

In 1969 a continuous air quality monitoring was initiated by the Health Authorities of Oslo. In 1970 this network consisted of 3 stations for daily measurements and 1 station for half-hourly measurements of SO_2.

For the purpose of the NILU air pollution study in 1970 and 1971, further measurements were required to provide adequate geographical coverage and to increase the time resolution of the measurements. 22 additional stations for daily measurements of SO_2 and suspended particulates (24h average), and 4 stations for half-hourly measurements of SO_2 were established by NILU.

This section of the report summarizes the data derived during the winter of 1970/71, with main emphasis on the SO_2-data. In addition, data from neutron activation analysis of filters are presented, to indicate the chemical composition of the suspended particulates in Oslo.

4.2 Monitoring network

The location of the stations for daily sampling is shown in Figure 4.1. The stations 1, 14 and 15 were run by the Health Authorities of Oslo and the station 12 by the oil companies.

The remaining stations were run by NILU. See Table 4.1.

The sites of the stations 1, 4, 7, 8 and 17 were for comparison purposes identical with the sites used in the period 1958-65.

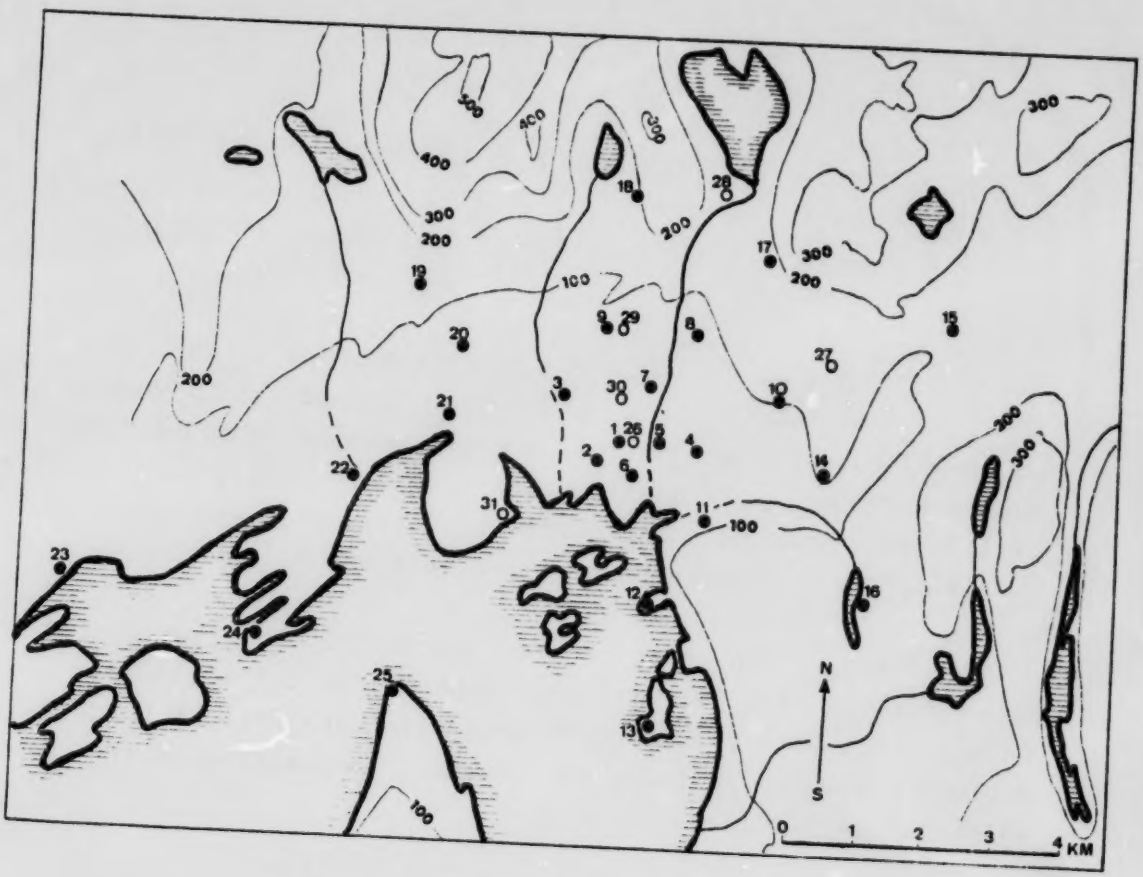

Figure 4.1: The air quality monitoring stations in Oslo 1970-71.

Station	Location	Height (m) a.s.l. of station	Description of location	Air volum m^3/day	Operated by	Monitoring period
1	St. Olavsplass	22	Commercial and offices	2.0	HA	30/9-70 - 20/4-71
2	Haakon VII's gt.	25	"	2.4	NILU	26/2-70 - 31/3-71
3	Briskeby	15	Commercial-residential	2.4	"	26/2-70 - 31/3-71
4	Heimdalsgt.	11	Industrial-offices	3.6	"	16/11-70 - 31/3-71
5	Mariboes gt.	16	Light industry-residential	3.6	"	28/1-71 - 9/3-71
6	Stortorget	14	Commercial and offices	3.6	"	3/12-70 - 9/3-71
7	Kingos gt.	41	Residential-light industry	2.4	"	30/9-70 - 31/3-71
8	Sagene	86	Industrial-residential	3.6	"	1/12-70 - 10/3-71
9	Ullevål sykehus	81	Residential-offices-hospital	3.6	"	4/12-70 - 19/4-71
10	Økern	94	Industrial	2.4	"	19/2-70 - 31/3-71
11	Ekeberg	143	Residential-school	2.4	"	8/10-70 - 31/3-71
12	Sjursøya	6	Industrial	3.6	"	3/1-71 - 9/3-71
13	Malmøya	7	Residential	3.6	"	30/12-70 - 9/3-71
14	Bryn	90	Industrial	2.0	HA	29/10-70 - 14/4-71
15	Hyland	125	Residential-offices	2.0	HA	29/10-70 - 14/4-71
16	Østensjø	136	Residential	3.6	NILU	30/12-70 - 11/3-71
17	Grefsen	195	Residential	3.6	"	16/11-70 - 31/3-71
18	Kringsjå	200	Residential	3.6	"	8/12-70 - 3/2-71
19	Huseby	141	Residential-schools	3.6	"	4/12-70 - 9/3-71
20	Smestad	58	Residential	3.6	"	8/12-70 - 9/3-71
21	Skøyen	12	Industrial-offices	3.6	"	3/12-70 - 31/3-71
22	Lysaker	54	Residential	3.6	"	22/12-70 - 9/3-71
23	Sandvika	7	Industrial-residential	3.6	"	22/12-70 - 9/3-71
24	Snarøya	6	Residential	3.6	"	4/12-70 - 9/3-71
25	Nesodden	19	Residential	3.6	"	3/12-70 - 17/3-71
26	St. Olavsplass	22	See 1	0.26	HA	
27	Vollebekk	127	Offices-residential	0.26	NILU	1/12-70 - 2/4-71
28	Kjelsås	142	Offices-residential	0.26	"	3/12-70 - 26/1-71
29	Ullevål sykehus	81	See 9	0.26	"	26/1-70 - 20/4-71
30	St. Hanshaugen	86	Residential	0.26	"	3/12-70 - 1/4-71
31	Sjøfartsmuseet (Bygdøy)	5	Residential	0.26	"	4/12-70 - 1/4-71

Table 4.1: Location and description of sampling sites.

HA: Health Authorities

Stations 1-25: SO_2 bubblers (24h average)

Stations 26-31: SO_2 continuous recording instruments, imcometer ($\frac{1}{2}$, $\frac{1}{4}$ h average).

The sampling time was from 14h to 14h local time at all stations. The different laboratories applied different instrumentation and analysis techniques. At NILU the samples were analysed by the Thorin-method, (8) and (9). W. Lindberg (1), the Health Authorities and the oil companies used the method established by OECD (10). The SO_2 monitoring measurements necessitate a proper control procedure, particularly since different methods are applied. Therefore, simultaneous concentrations of SO_2 were correlated for each month. The results from the correlations were evaluated on the basis of the experience from similar controls of the data in the period 1959-65 (1), (3). Figure 4.2 shows an example of spatial correlations. If the data from a station gives significantly lower correlation than expected with the other stations, strong influence from nearby sources or errors in sampling and chemical analysis may be suspected.

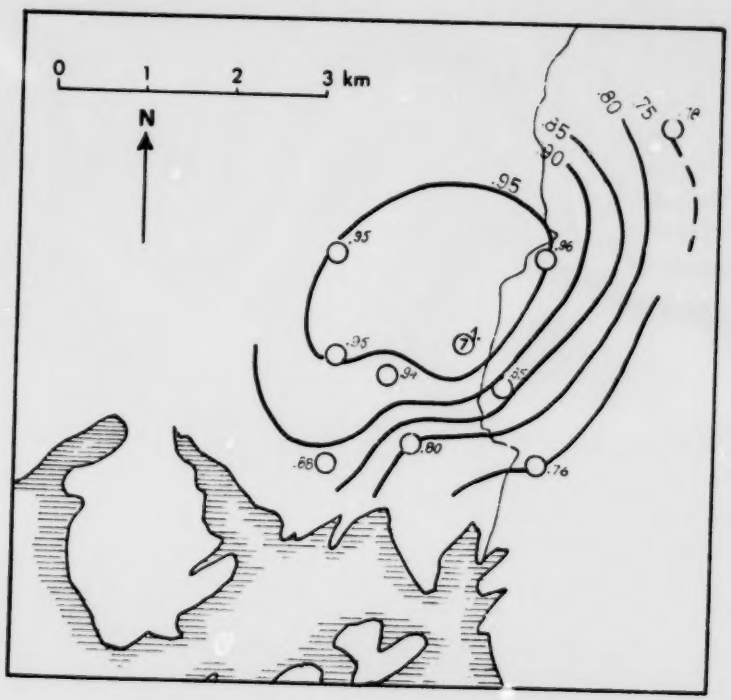

Figure 4.2: SO_2 concentrations at station 7 correlated with other stations. 1959-63, weeks 2-10.

Whatman filters no 1 were used at all stations. The amount of total suspended particulates was estimated by means of the reflectometric method (OECD standard method 1964 (10)). The use of the proposed international standard calibration curve implies an uncertainty in the absolute values. This must be considered when interpreting the measurements of suspended particulates.

Determination of half-hourly mean values of SO_2 were made at 6 sites in Oslo. The station 28 was in operation only during December and January and station 29 in February and March. An automatic gas analysis instrument, (Imcometer, produced by Bran and Lübbe) was used. The analysis is based on the West and Gaeke method with pararosaniline as colourreagent. The examination of the data showed much noise in the half-hourly measurements. Hence hourly mean values of SO_2 were used in the data processing. This time resolution was found convenient regarding the model approximations.

4.3 Results

A. SO_2 and suspended particulates

The air quality data presented in this report cover mainly the winter 1970/71 during the period with extensive field studies (1st December through 15th March).

In Figure 4.3 the monthly mean values of SO_2 and suspended particulates are shown for all stations.

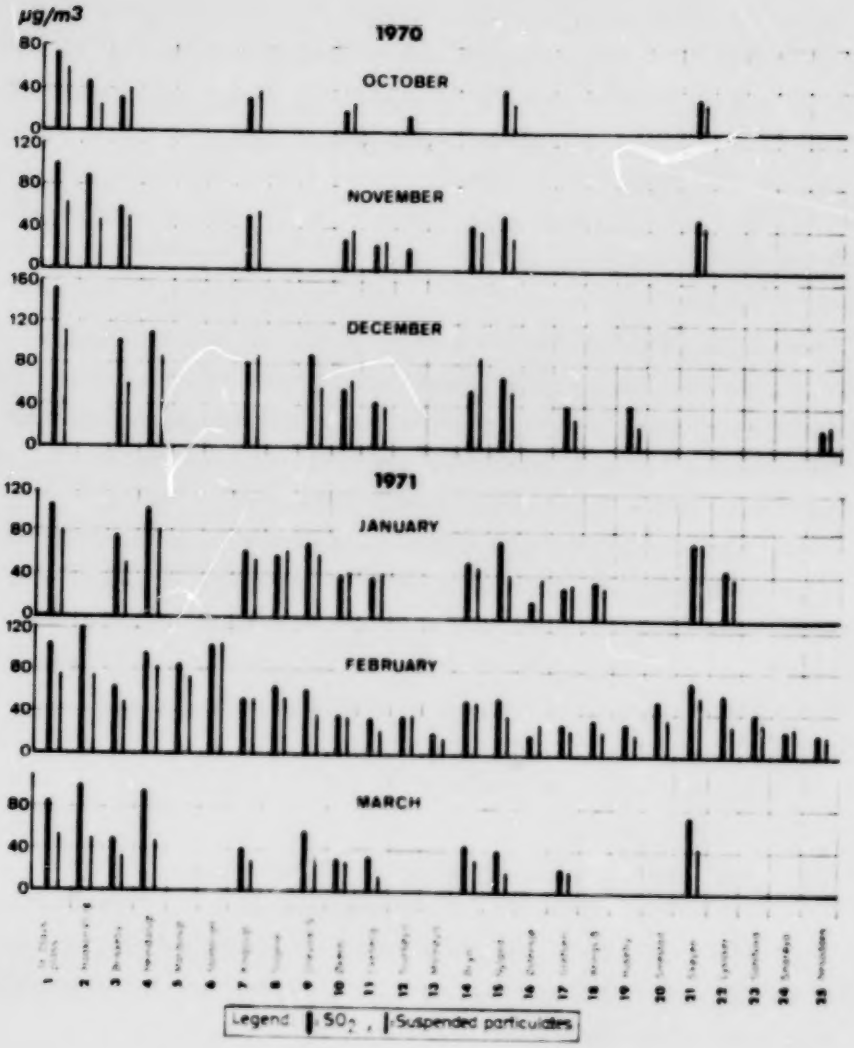

Figure 4.3: Monthly mean values of SO_2 and suspended particulates, winter 1970/71.

In Norway the ambient SO_2 concentrations are normally compared with the Swedish air quality standards. The Swedish standard (11) for monthly mean concentrations (140 µg SO_2/m^3) was exceeded only in December, and for daily mean concentrations (280 µg SO_2/m^3) only one day.

The US-primary standard for daily mean concentrations of SO_2 (365 µg $/m^3$) was not exceeded, whereas the secondary standard (260 µg/m^3) was exceeded 2 times (days in December and January) in the centre of the city (12). The US-primary standard for suspended particulates (260 µg/m^3) was exceeded 6 times (days) in the centre of the city. The secondary standard (150 µg/m^3) was exceeded frequently (52 times at 6 low elevation stations) during the months December through February. The maximum daily mean SO_2concentration was 349 µg/m^3 (station 1), and the maximum concentration for suspended particulates was 493 µg/m^3 (station 4).

The annual mean SO_2 concentration for the centre of the city (station 26) was 100 µg (July 1970 - June 1971), which exceeded the primary US-standard (80 µg SO_2/m^3).

Figure 4.4 a) shows the distribution of monthly mean values of SO_2 in February, and Figure 4.4 b) the mean values for a period (3-6th February) with heavy air pollution (temperature inversion). In the centre of the city the SO_2 concentrations during the inversion were approximately twice the monthly mean becoming gradually lower towards the suburbs.

Figure 4.5 shows the mean diurnal variation of the SO_2 concentration in January 1971 for stations 26, 30 and 31 (data from December and February was not used due to incomplete data at station 30). Data for all three months are given for stations 26 and 27.

Figure 4.4 a) Monthly mean concentrations of SO_2 in February 1971 in Oslo. Units: µg SO_2/m^3 air.

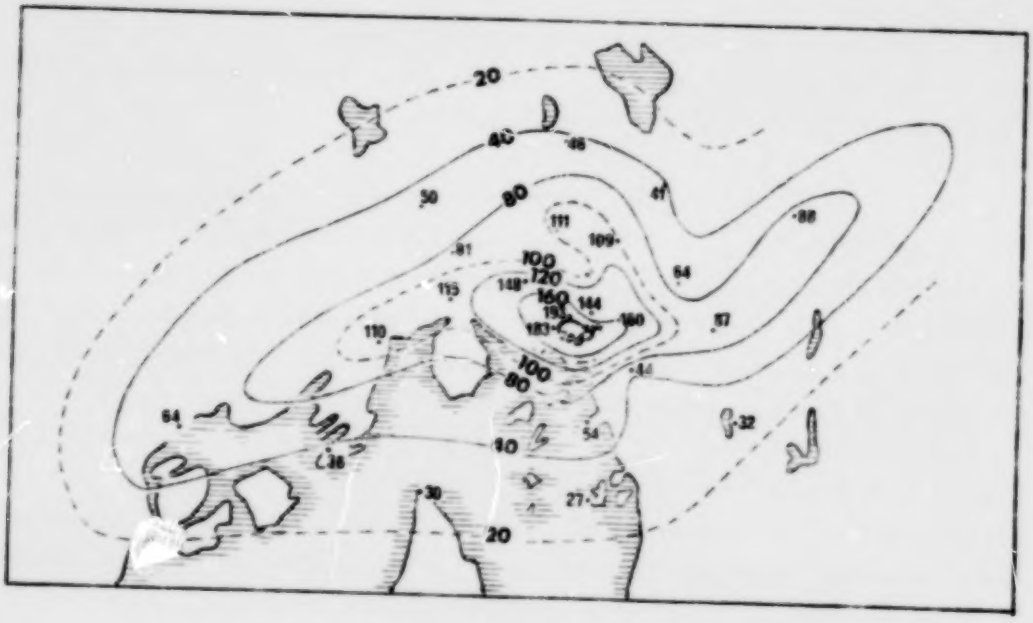

Figure 4.4 b) Mean concentrations of SO_2 3-6 th February 1971. Units: µg SO_2/m^3 air.

At station 30 (situated on a hill 80 meters a.s.l.) the maximum concentration occurred 3 hours later than at station 26 in the centre of the city. At station 31, furthest to the south, the maximum occurred earlier than at station 30. This pattern is also reflected in the corresponding data from December and February. This difference between the stations is probably due to the combined effect of the increased emission in the centre of the city and the onset of onshore wind during daytime.

Also at station 27, located in the suburb, the maximum of the hourly mean concentrations for the period December 1970 through February 1971 occurred at daytime (11h). (See also paragraph 6.4).

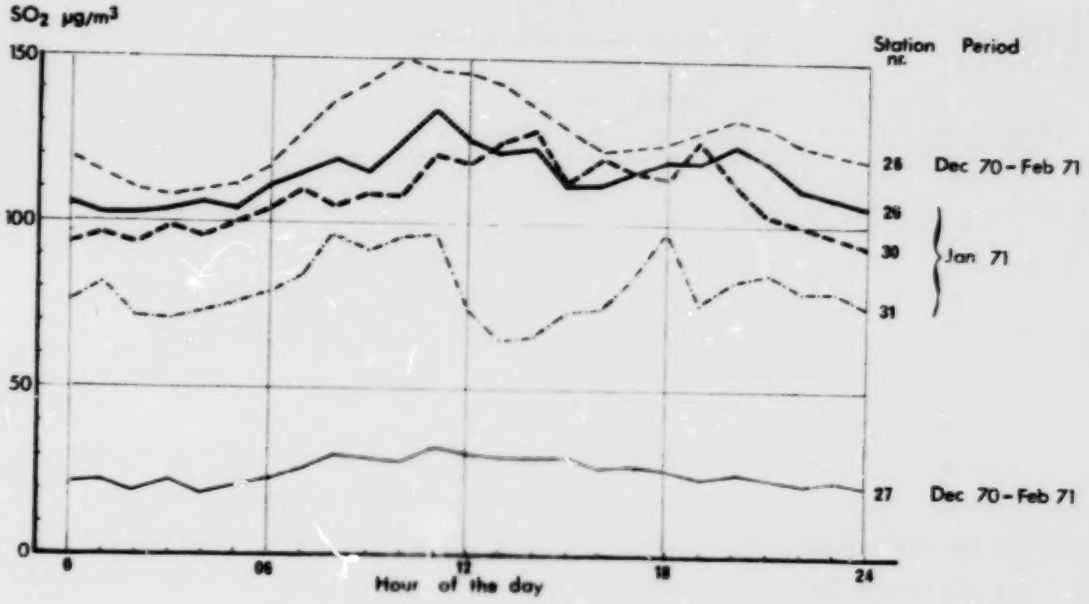

Figur 4.5: Mean diurnal variation of the SO_2 concentration at the stations 26 (St. Olavsplass), 30 (St. Hanshaugen), 31 (Sjøfartsmuseet, Bygdøy) and 27 (Vollebekk) during the winter 1970/71.

Figure 4.6 shows the percentage of days at station 26 on which the maximum SO_2 concentration occurred during each specified 2 hour period. This does not distinguish between days with low and high pollution levels. In other cities the trends are similar (13) with the minimum frequencies in the afternoon and after midnight, and maximum during the daytime and in the evening. The evening and morning peaks are considered to be

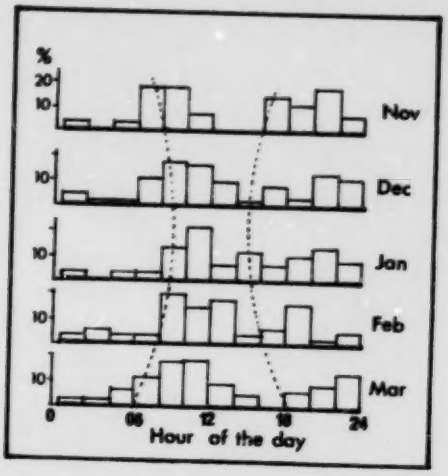

Figure 4.6: Percentage of days with maximum SO_2 values within specified 2 hour periods. Data from station 26 for the winter seasons 1969/70 and 1970/71 are used. Dotted lines mark sunrise and sunset.

caused primarily by increased emission rates. As distinct from other cities (e.g. Stockholm), high frequencies of maximum values also occurred several hours after sunrise, particularly in February and March. This may be due to local meteorological effects. During inversion situations in February it has been repeatedly observed that the instabilization of the air is not strong enough to break up the night-time inversion. During the night-time the down-

valley air flows are well defined. During the day-time the downvalley air flows gradually become weaker due to the increasing on-shore wind effect. Around noon, stagnation of the air or weak on-shore wind is genereally observed on days with inversions.

Figure 4.7 shows the variation through the week of the daily SO_2 mean concentrations on the average for the winter months 1970/71 at the stations 26 and 30 in the centre of the city. The weekly variation through the winter 1969/70 (not shown) was similar. The mean curves should give an indication of the weekly variation in the fuel consumption. This suggests that emission rates should also be a function of the weekday. A surprising result is that the mean value for Mondays is comparable in magnitude with the values for Saturdays and Sundays. However, mean values for a longer series of data is necessary to obtain reliable mean values.

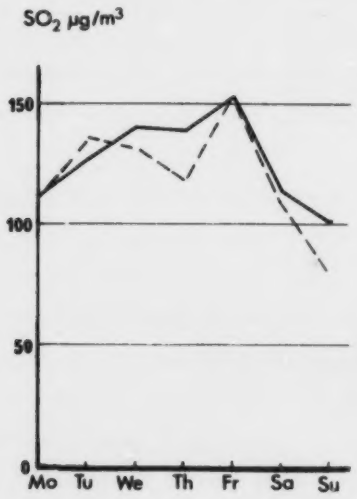

Figure 4.7: Weekday mean values of SO_2, December 1970 through February 1971.
_____ station 26 (St. Olavsplass)
-------- station 30 (St. Hanshaugen)

B. Elements in particulate matters

The amount of different elements on all filters for six selected days have been determined by means of neutron activation analysis. The metals being determined were Fe, Mn, Zn, Br, Cu, Ti, Al, V, Cr, Sb.

In figure 4.8 are as examples presented the area distributions of

a) the total of suspended particulates (reflectometric method),
b) vanadium
c) iron for 5-6th of February 1971

During 5-6th February the wind was weak and shifty and mainly from northerly and north-easterly directions and the stratification of the air was stable. The distribution of particulates and vanadium had an eastnortheast - westsouthwest axis with a maximum concentration in the centre of the city, whereas the distribution of iron had a northnortheast - southsouthwest axis with a maximum in the northern part of Oslo.

The concentrations of the different elements were correlated. The area distribution of iron was well correlated with manganese (R = 0.93), zinc (R = 0.86) and chromium (R = 0.80), whereas the correlation with suspended particulates was lower (0.68). The area distribution of vanadium was best correlated with SO_2 (R = 0.61) and suspended particulates (R = 0.50). Bromine (Br) was the element best correlated with suspended particulates (R = 0.87) at 5-6th of February.

Figure 4.8: Distribution, in Oslo on 5-6th February, of
a) suspended particulates ($\mu g/m^3$),
b) vanadium ($\mu g/m^3 \cdot 10^{-2}$) and
c) iron ($\mu g/m^3$).
Weather: Stable stratifications, weak northerly wind.

Stations	Date	Fe	Mn	Zn	Cu	Ti	V	Cr
8 Sagene	5-6 2 11-12/2	33.9 0.7	3.6 0.04	15.9 0.4	0.02 0.03	0.4 0.4	0.029 0.021	0.090 0.010
6 Stortorget	5-6/2 11-12/2	11.4 1.1	3.1 0.04	7.2 0.2	0.3 <0.02	<0.1 <0.2	0.051 0.021	0.092 0.013
11 Ekeberg	5-6/2 11-12/2	0.2 1.7	0.02 0.03	0.2 0.2	0.05 0.09	<0.1 <0.1	0.003 0.001	<0.005 <0.005
US values	Site Year Max 90 percentile	Johnstown Penn. 1963 16.0 4.9	Johnstown Penn. 1963 6.9 2.38	Portland Oregon 1963/64 4.8 1.76	New York city 1957 1.8 0.87	San Bernadino Calif. 1963 0.21 0.10	Tampa Florida 1963 0.085 0.056	Rochester New York 1960 0.290 0.095

Table 4.2: Daily mean concentrations i $\mu g/m^3$ of elements in suspended particulates at three stations in Oslo for two selected days. The highest daily concentration measured in US (urban) and the 90 percentile of the measured concentrations at the same location (14) are included for comparison.

In Table 4.2 are presented the data for two days with different weather conditions. 5-6th of February represents a day with stable and stagnating air in Oslo (Figure 4.8). 11-12th of February represents a day with unstable to neutral stability of the air and relatively strong wind (2-6 m/s) from south to southwest. The data from three stations are used; station 8 situated in a residential area about 1.2 km south of a steel work and a galvanizing plant; station 6 in the centre of Oslo and station 11 near the city centre, but situated on a hill approximately 140 meters a.s.l.

The lower part of table 4.1 gives the highest daily concentrations measured in urban areas in USA (14) and the 90 percentile of the concentrations measured at the same locations. Table 4.1 shows that extremely high concentrations of Fe and Zn may occur in Oslo, compared with maximum values measured in USA. Also the measured concentrations of Mn, Cu and Ti are very high compared with measurements from the US, whereas the concentrations of V are relatively low.

Comparison of the two selected days, with respect to their different weather conditions, show great variation in the concentrations of especially Fe, Mn and Zn at the stations 6 and 8. This, together with the Fe-distribution shown in Figure 4.8, and the results from the correlation analysis, indicate a dominant source in the northern part of Oslo.

The high concentrations of Fe (and Al) for station 11 (and the neighbouring stations towards northeast) on 11-12th of February are probably caused by a local source.

4.4 Concluding remarks

Only one monthly mean value (December) and one daily mean value for SO_2 exceeded the recommended standards for Sweden, during the winter 1970/71. Favourable dispersion conditions were prevailing during this winter.

The concentrations of suspended particulates did exceed both the US-standards for hourly mean concentrations, and the secondary standard was exceeded relatively often. Regarding the content of iron and zinc in the suspended particulates, extremely high values have been observed in the air in Oslo. The spatial distribution indicates one dominant source in the northern part of Oslo.

The statistics for the diurnal variation of the SO_2 concentrations show that the mean SO_2 concentration was highest in the middle of the day, and that the probability of observing the maximum concentrations during the night and the afternoon was low (Figures 4.5 and 4.6).

5 METEOROLOGICAL MEASUREMENTS

5.1 Introduction

In this study meteorological data collected during the winter 1970/71 were used. The stations are shown in Figure 5.1 and listed in Table 5.1. Three of the stations, Fornebu (A), Oslo (Blindern) (B) and Tryvasshøgda (H) are official stations run by the Norwegian Meteorological Institute (MI). NILU operated 7 wind stations and 7 thermograph stations. Four of the thermograph stations (D, E, F, G) were placed along one of the hillsides, in order to obtain a measure for the thermal stability. The heights of the stations are given in Table 5.1. One thermograph station was placed in the centre of the city to record the heat island effect.

Fuess thermographs and Lambrecht Woelfle windrecorders were used. At the permanent meteorological stations Fornebu and Blindern, Fuess 90Z windrecorders are used. This recorder has a higher starting threshold than the Woelfle recorder (about 1.0 and 0.4 m/s respectively). The windrecordings were made at a height of 10 meters above the ground, except at Blindern (B) (26 m), Nydalen (O) (20 m) and Sentrum (K) (40 m above street level). The temperature and wind were recorded as hourly mean values.

Special recording programs were carried out during 11 air pollution episodes.

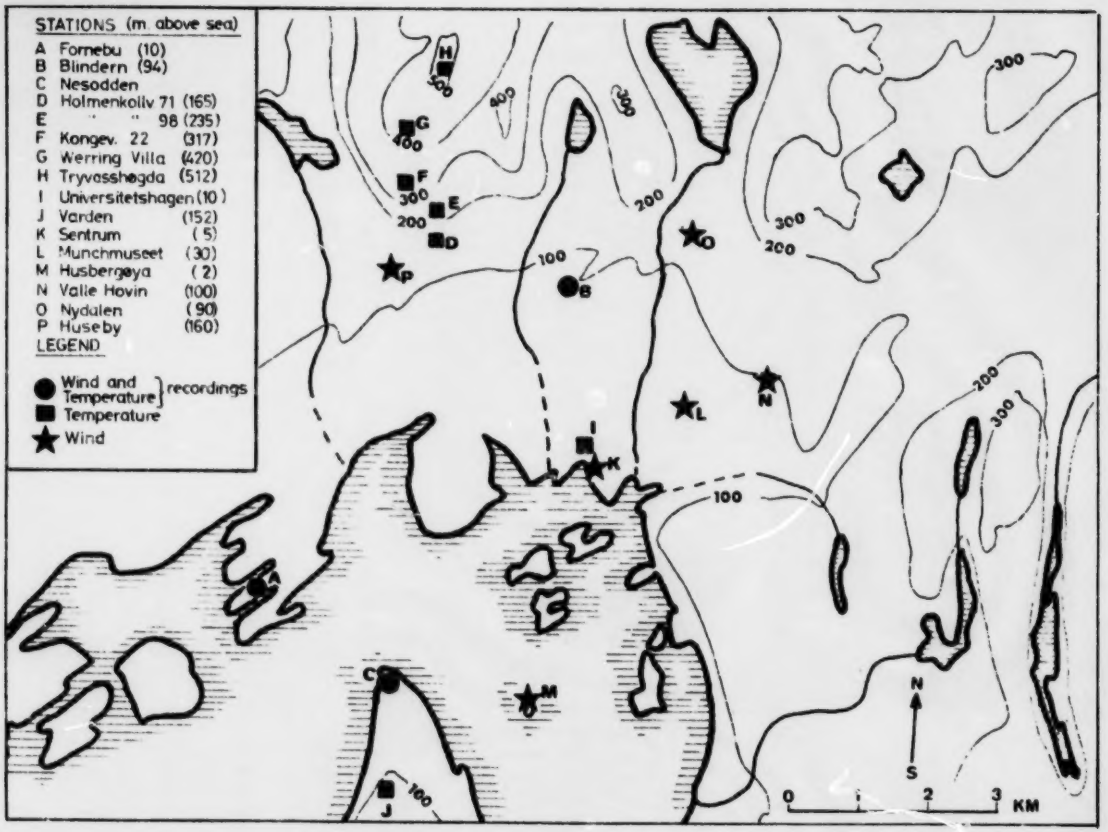

Figure 5.1: Meteorological stations.

Station	Location	Height (m) a.s.l. of station	Height above ground	Operated by	Type of instrumentation and frequency of observation	Monitoring period
A	Fornebu	10	11(F), 2(T)	MI	T F 1h	cont
B	Oslo (Blindern)	94	26(F), 2.2(T)	MI	T F 2h	cont
C	Nesodden	15(W), 3(T)	10(W), 2(T)	NILU	T W 1h	27/11-70 - 10/3-71
D	Holmenkollvn. 71	165	2	"	T 1h	26/11-70 - 15/3-71
E	Holmenkollvn. 98	235	2	"	T 1h	26/11-70 - 15/3-71
F	Kongevn. 22	317	2	"	T 1h	26/11-70 - 15/3-71
G	Werrings villa	420	2	"	T 1h	26/11-70 - 15/3-71
H	Tryvasshøgda	512	2.1	MI	Obs 07 13 19	cont
I	Universitetshagen	10	2	NILU	T 1h	27/11-70 - 15/3-71
J	Varden	152	2	"	T 1h	24/11-70 - 18/3-71
K	Sentrum	5	40 (Roof)	NILU	W 1h	12/2 -70 - 10/3-71
L	Munch-museet	30	10	"	W 1h	27/11-70 - 10/3-71
M	Husbergøya	2	10	"	W 1h	9/2 -70 - 10/3-71
N	Valle Hovin	100	10	"	W 1h	7/2 -70 - 10/3-71
O	Nydalen	90	20	"	W 1h	10/2 -70 - 10/3-71
P	Huseby	160	10	"	W 1h	9/2 -70 - 12/1-71

Table 5.1: Location and description of meteorological measurement.

T = Thermograph

F = Wind recorder Fuess 90Z

W = Wind recorder Lambrecht Woelfle

Obs: Instrumental observations.

During the air pollution episodes three cars followed selected routes for the measurement of wind and temperature at a great number of locations. The temperatures were measured with a resistance thermometer placed on the roof of the car. Temperature readings could be made from the inside of the car moving at a specified speed (40 km/h). The wind-observations were made by observing the drifting directions of the chimney plumes, and also by observing drifting soapbubbles. The last method could be used because low windspeeds were associated with the pollution episodes. The soapbubbles could be seen up to a distance of approximately 50 meters. The wind speed was taken as the speed of the soapbubble.

For the observation of the vertical variation of the wind and temperature, pilot balloons were launched from up to 6 positions and wiresonde and radiosonde observations were made from the roof of a building in the centre of the city. In addition, timelapse photography was done at three different points with good views of Oslo.

5.2 Average meteorological conditions.

The meteorological conditions for the winter 1970/71 was compared with the "normal" conditions by means of data from the permanent stations, run by the Norwegian Meteorological Institute.

A. Wind

To compare the wind conditions during the winter 1970/71, with the "normal" conditions during the winter, the windroses for December through February for the winter 1970/71 and for the period 1931-60 at Blindern (B) (16) are shown in Figure 5.2. The most frequent wind direction is from NE. The main features of the windrose for the winter 1970/71 are similar to the 30-year mean windrose for the same months.

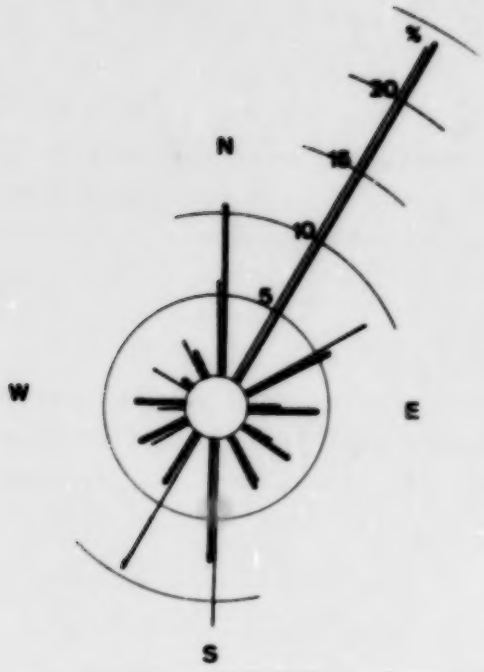

Figure 5.2: Windfrequencies for Blindern (B) for December 1970 through February 1971 and the period 1931-60.

——— Winters 1931-60 (Calm: 28.2%)
——— Winter 1970/71 (Calm: 24.4%)

Wind Speed Range (m/s)	Frequency (%)
< 3	80
3 - 8	17
> 8	3

Table 5.2: The frequency distribution of wind speed observations in Oslo 1941-50, December through February.

The windflow is generally weak during the winter (Table 5.2), with a mean wind speed of 1.9 m/s. For 1970/71 the mean wind speed at station B was approximately 2.0 m/s.

B. Temperature

Table 5.3 presents the average temperature for each winter-month for the years 1931-60 (15) and for the winter 1970/71. It appears that 1970/71 was much warmer than the normal.

	1931-60	1970/71
December	-2.0	-1.4
January	-4.7	-2.4
February	-4.0	-0.5

Table 5.3: Average monthly temperatures. Unit: ^{o}C.

C. Atmospheric stability

In Table 5.4 the mean monthly frequencies of inversions in the period from 1958/59 through 1967/68 is compared with the corresponding frequencies in 1970/71. The frequency of inversions is defined as the number of days when the temperature at 07h was higher at Tryvasshøgda (H) than at Blindern (B). The table shows that the monthly mean frequencies for the period 1958/59 - 1967/68 are higher than in 1970/71 for all three months, particularly February.

Winter periods	December	January	February
1958/59 - 1967/68	10.0	11.5	10.5
1970/71	8	7	5

Table 5.4: Monthly frequencies (number of days) of inversions in Oslo (based on temperature observations at 07h).

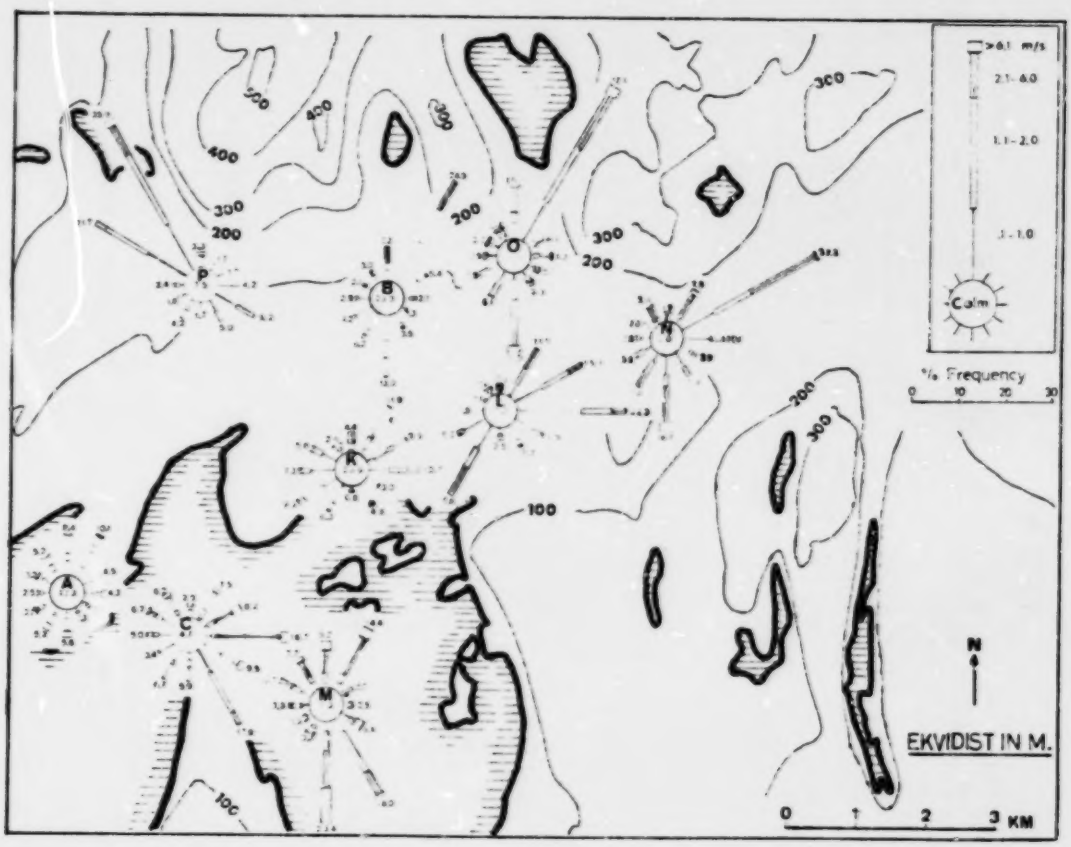

Figure 5.3: Windroses for December through February 1970/71 for the stations in Oslo.
Station P: 1. December - 12. January.

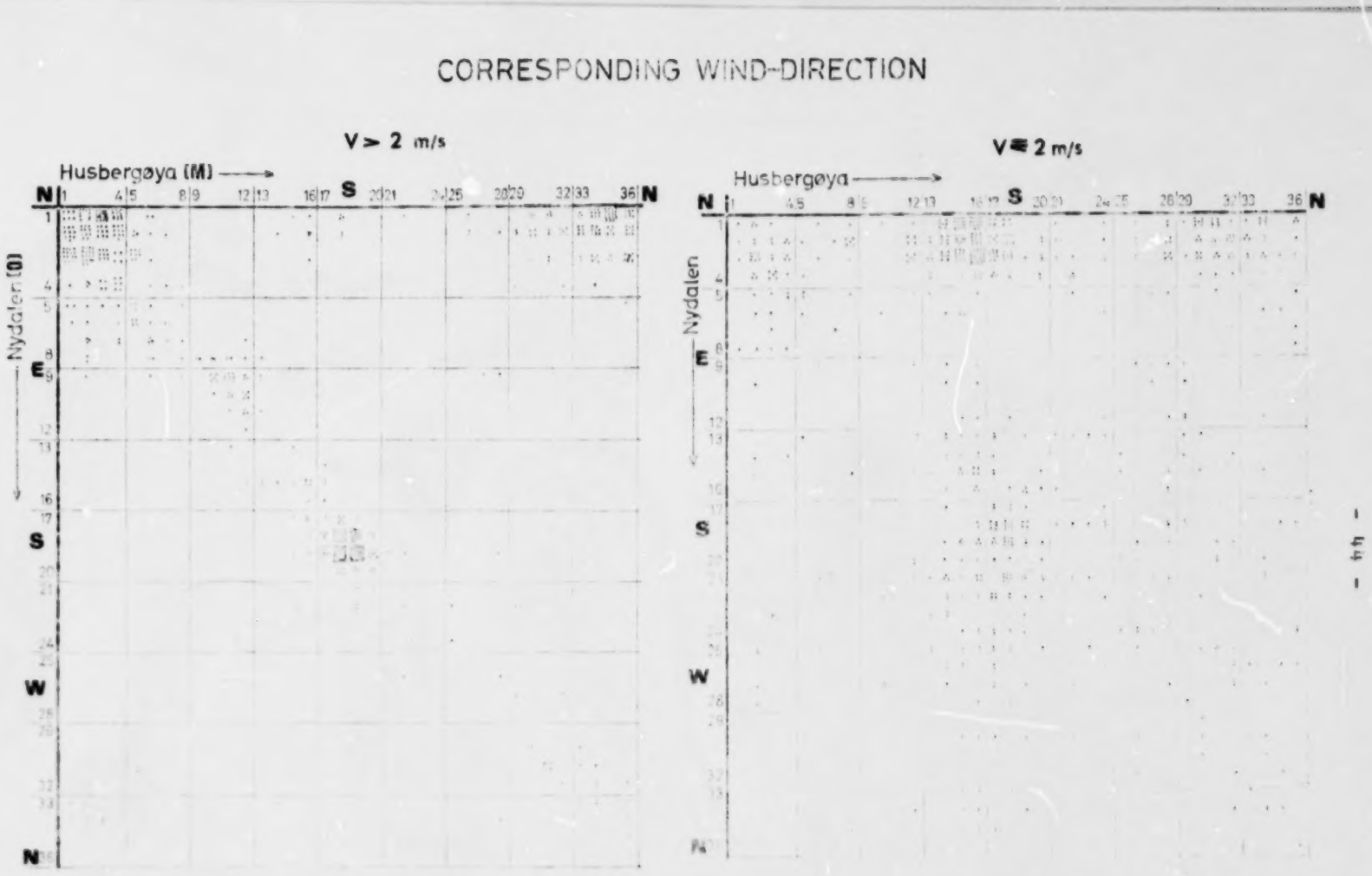

Figure 5.4: The relation between corresponding wind directions at the stations M and O during the winter months December through February, with wind speeds above and below 2 m/s.

Reproduced from best available copy.

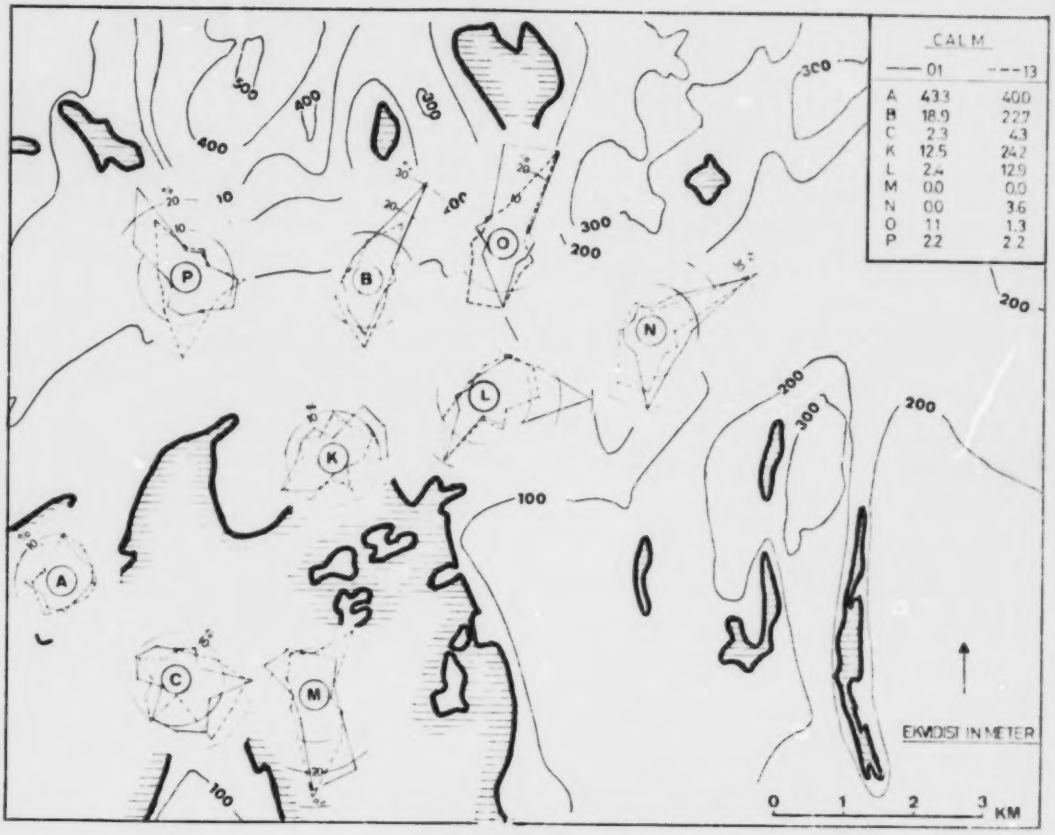

Figure 5.5: Windroses for December through February for 01h and 13h local time.
Station P: September through November 1970.

5.3 Results - Meteorological data 1970/71

A. Wind

The windroses for all wind stations in Oslo for December through February 1970/71 are shown in Figure 5.3. Station P

was only in operation until 12. January 1971.

At the suburb stations located in the west, north and east of the centre of the city, the prevailing wind directions were towards the fjord. In the city centre (station K) the wind distribution was complex. It is an interesting fact that on "fjord stations" C and M southerly winds prevailed, whereas on station A northerly winds seemed to be prevailing. However, the very high frequency of "calm" on this station (high starting threshold of the windrecorder) reduces the representativity of this wind distribution.

Considering only the occurrence of weak winds ($\leq$ 2 m/s), the windroses show that on all stations, except station K in the centre of the city, the wind directions towards the centre of the area prevail. This is a typical wind distribution during periods with heavy air pollution. In Figure 5.4 this fact is demonstrated by means of the statistics of corresponding wind directions for the "fjord station" M and the "land station" O, for wind speeds higher and lower than 2 m/s. For wind speeds (at station O) higher than 2 m/s the directions are generally the same. For windspeeds lower than 2 m/s, the relation is rather complex. It is, however, clearly shown that with weak winds from NNE in the northern part of the city (O), the most probable wind direction is from SSE in Bunnefjorden (M), i.e. the air flows towards the centre of the city at both stations.

During conditions with low wind speeds, the dominating wind system and circulations are generated by thermal non-uniformities of the underlaying surface, such as land-sea temperature

difference, different heating by sun radiation, heat island effects and (nocturnal) gravitational flows.

The local effects have a diurnal variation. In Figure 5.5 the windroses for 01h and 13h for the period December through February are presented for all stations. For station P, however, the windroses for the period September through November 1970 are applied. The diurnal variation of the wind was pronounced at the suburban stations B, N, O, P and at the station L. At the stations K and L the different frequencies of "calm" at 01h and 13h may obscure the variation. At the "fjord stations" there was no pronounced diurnal variation. At station A (Fornebu) the very high frequency of calm wind conditions (or wind speeds below the starting threshold, about 1.0 m/s) may also here have obscured the diurnal variation of the winds.

B. Temperature and thermal stability

The purpose of the temperature measurements were to describe the stability conditions, the heat island effect (5.3C) and the mixing height (5.3D).

Thermal stability

The thermal stability conditions were studied by means of temperature recordings from the stations A, B, D, E, F, G, H and I, situated at different heights. The purpose of the investigation was to find the typical inversion heights for the Oslo area, and to evaluate the representativity of the temperatures observed at the standard observation hours at the permanent MI-observations (stations A, B, G) with respect to inversion frequencies for the Oslo area.

To study the variation of the inversion height, the number of times the maximum temperature of the thermograph chain was observed at individual stations, was counted, i.e. the inversion height was defined to be equal to the height a.s.l. of the station with the highest temperature. This was also assumed to apply to situations with multilayer inversions. All hourly observations (2160) were applied. Station H was omitted because observations were made only 3 times a day. With this method, the frequencies of inversions are overestimated because only the maximum values are counted. The results are presented as cumulative graphs in Figure 5.6; with the stations Fornebu (A) and Universitetshagen (I) (in the centre of the city) as the lowest. The graph should not be used indiscriminantly, but it does, however, give a fairly good estimate of the variation of the frequency with height.

Curve 1 indicates that inversions occured 64% of the total time and that half of the inversions occurred below a height of approximately 100 m (station B). It must, however, be kept in mind, that the temperature difference between station A and station B may be influenced by a horizontal temperature difference over the distance of 10 km between the stations. The difference between curve 1 and 2 may be explained by the fact that station I (Universitetshagen), located at a distance of 3 km from Blindern (B), was situated within the city heat island. Therefore, the temperature at Fornebu (A) may be taken as fairly representative of the temperature of the lower level of the Oslo area.

Above station B, the top of the inversions were most frequently located around the height of station F (317 m). As a consequence, the air pollution potential decreases significantly with height, particularly above the first 100 meters.

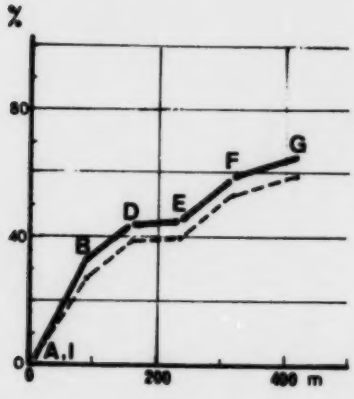

Figure 5.6:
The percentages of the total of hourly observations in December through February 1970/71 with a stably stratified layer of air only below the different thermograph stations.
I —— Lowest station Fornebu (A)
II---- Lowest station Universitetshagen (I).

When relating air pollution to meteorological conditions it is convenient to use one single temperature difference between two stations as a stability parameter. The temperature difference at 07h between the permanent MI stations B (Blindern) and H (Tryvasshøgda) has been used as the stability parameter. In Table 5.5 the inversion frequencies for the observation hours 07, 13 and 19h in the period December 1970 through February 1971 are given for some selected station pairs. The observations at 07h and 19h may be considered as night observations during these months.

Station pair	B - H	A - B	A - F	B - F
Heights (m)	94 - 512	10 - 94	10 - 317	94 - 317
Inversion frequency in %	21	54	32	29

Table 5.5: Inversion frequencies, based on temperature differences between different station pairs during the months December 1970 through February 1971. Time of observations 07, 13, 19h.

The frequency of "inversions" between the stations A and B was close to the total of inversions below station G (see Figure 5.6). Considering the inversion frequencies above the station B (Blindern), a difference of 8% is observed between the permanent station pair B-H and the pair B-F.

The frequency of inversions between Blindern (B) and Tryvasshøgda (H) for the observation hours 07, 13 and 19h was slightly less than the frequency based on the observations at 07h (22%, see Table 5.4). It may be concluded that the inversion frequency for Oslo is underestimated by using the temperature difference between the stations Blindern (B) and Tryvasshøgda (H), and that an additional station at a level of 300 to 400 m a.s.l. should be used for this purpose.

C. The heat-island

The temperature difference between the centre of the city (station I) and the surroundings (station A) was used to measure the heat island effect in Oslo. The mean values of these differences for each hour of the day during the winter 1970/71 are shown in Figure 5.7 (curve $\overline{\Delta T}_{I-A}$). This figure shows that during the night the temperature in the centre of the city is about 0.70 - 0.80°C higher than in the surrounding area. This mean difference becomes smaller between 10h and 18h with a minimum heat island effect at 14h. This pronounced minimum coincides with the typical maximum of the instability during the daytime.

The dependence of the urban heat island effect on meteorological conditions was investigated by a multiple regression analysis. The results show a relationship between the vertical temperature gradiant outside the urban area and the temperature excess of the heat island.

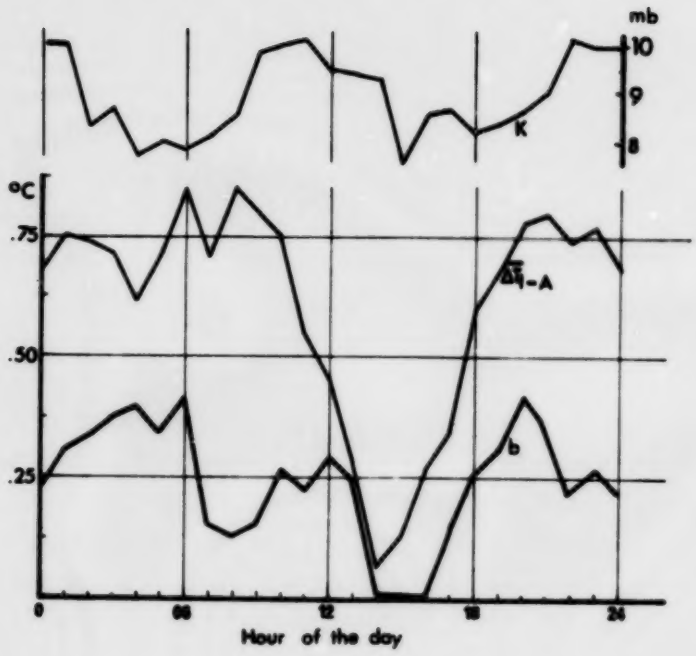

Figure 5.7: The daily variation of the urban heat island effect ($\overline{\Delta T}_{I-A}$) and its dependence on the vertical temperature stratification (γ) in Oslo during the winter 1970/71. The values of the coefficients K and b in the regression equation $\Delta T_{I-A} = b - K\gamma$ for each hour of the day are presented.

The regression equation may be written:

$$\Delta T_{I-A} = b - K\gamma \qquad \text{(Eq 5.1)}$$

ΔT_{I-A} = The temperature difference between the centre of the city (station I) and the surrounding area (station A).

γ = The vertical temperature variation with pressure $^{o}C/mb$. The temperature difference between the stations A and G was used.

The relatively high correlation between ΔT_{I-A} and γ (R=0.75 as an average for all hours) indicates that the vertical lapse rate changes with the physical processes which generate the heat island effect in Oslo. The diurnal variation of the regression coefficient K and the constant b should be dependent on the mean diurnal variation of the physical processes involved (see below).

Many interacting effects are involved in the formation of a heat island. Some of the effects are; emissions of heat and pollution, thermal radiation from the pollution cloud, different heat capacity of the ground and the buildings, difference in absorption of sun radiation between the city centre and the suburbs, the mean variation in the ventilation of the air, sea/air interaction, etc.

When considering the important effects in Oslo, it should be noted that the whole area was covered by snow, that the sun's elevation was low (most of the time less than 10°), and that the urban heat source due to the human activity is at a maximum during winter.

The coefficient (K) has a typical diurnal variation with one maximum in the middle of the night and one in the middle of the day (Figure 5.7). The coefficient fluctuates between 8 and 10 mb in a systematic way and does not exhibit random variation. The regression constant b, giving the mean heat island effect during weather situations with isothermal stratification, varies in the hourly analysis between 0.0 and 0.4°C (Figure 5.7). The value of b indicates that a very small heat island effect will be observed in the afternoon (14h - 16h) during isothermal stratification conditions, and the value of K implies that strong heat islands may also occur in the afternoon with strong inversion conditions.

The difference in the diurnal variation of the heat island effect during strong inversions (curve K) and isothermal conditions (curve b) should be due to a variation of the physical processes with the meteorological conditions.

The minimum value of b during the day indicates that the contribution from solar radiation to the formation of a heat island is not important when the vertical stratification is isothermal.

Strong inversions are associated with stagnant air, which prevents the dispersion of pollution and heat from the human activity in the urban area. The human activity is at a maximum during the day, and an increased heat island effect is observed about noon, when an inversion exists (see curve K in Figure 5.7). This may be attributed to the increased emissions of heat and pollution into the urban atmosphere. The maximum in the heat island effect during the night may be due to differences in the thermal properties between the urban surface (house-walls and ground) and the rural surface with respect to rate of cooling and heating. These results are in accordance with the results from other investigations (17).

D. The mixing height

A mixing height for the air pollution over Oslo may be defined from temperature recordings at the stations G, I and A. The mixing height is defined as the height of the intersection between the dry adiabat from the temperature in the centre of the city (station I) and the actual temperature profile (estimated from the temperature measurements at the stations A and G).

The hourly mixing heights were calculated for the period 1.12. 70 - 28.2.71, for days when a heat island effect existed (about 40 days). The Figure 5.8 shows the period average of this mean value of the mixing height for each hour through the day. Two things should be noted from this figure.

1. A diurnal variation is observed.

The mixing height is lower during the day than during the night. This is generally because the heat island is weaker during the day than during the night. If one assumes that an increase in the vertical mixing results in a decrease in the heat island effect, then the definition of the mixing height given above is certainly of limited value.

2. The mixing height appears to fluctuate with a period of about four hours.

This periodicity was also observed on single days, but it is difficult to identify the fluctuations in the individual temperature measurements (stations A, I, G). Different periodicities in the different temperature measurements may give a four hour period in the calculated mixing height. To study these fluctuations further, their connection to the wind-field should be investigated.

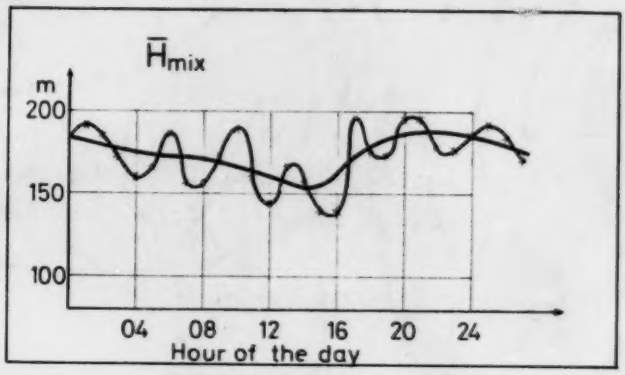

Figure 5.8: The diurnal variation of the mixing height. Hourly mean values for the period December 1970 through February 1971, from days when a heat island existed.

5.4 Results from the case studies

In order to present the results of the case studies of the local winter circulation during periods with a weak large-scale wind field, one of them (6.1.71) is selected as being representative.

Only the results from this case study is presented in detail. First, some comments are made on the synoptic weather situations where local circulations become important. The local wind- and temperature fields and their variation with height are described separately.

A. The synoptic situation

The synoptic situation is indicated on Figure 5.9 by a simplified version of the weather map from 6.1.71, 12.00 GMT. A high pressure area existed over the southern parts of Sweden and Norway. On the 5th of January, the centre of the high

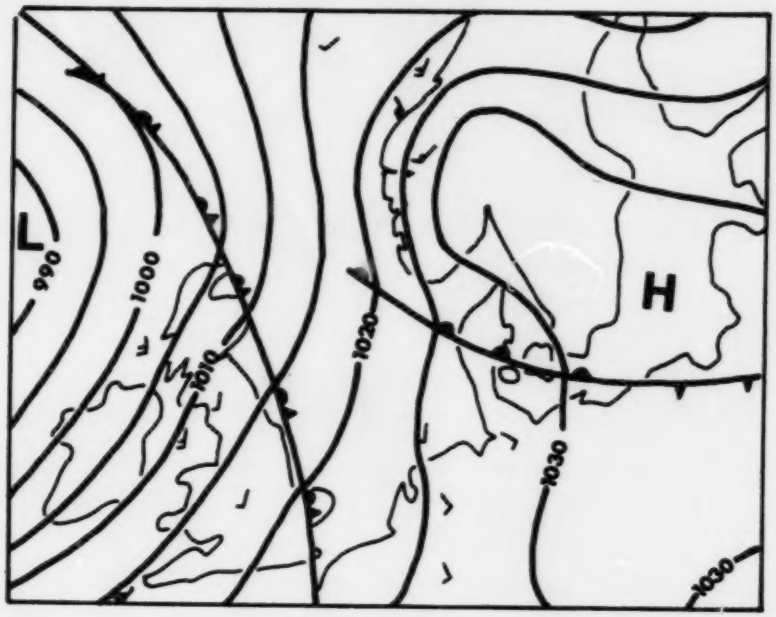

Figure 5.9: The weather map for Europe from 6.1.71. 1200 GMT.

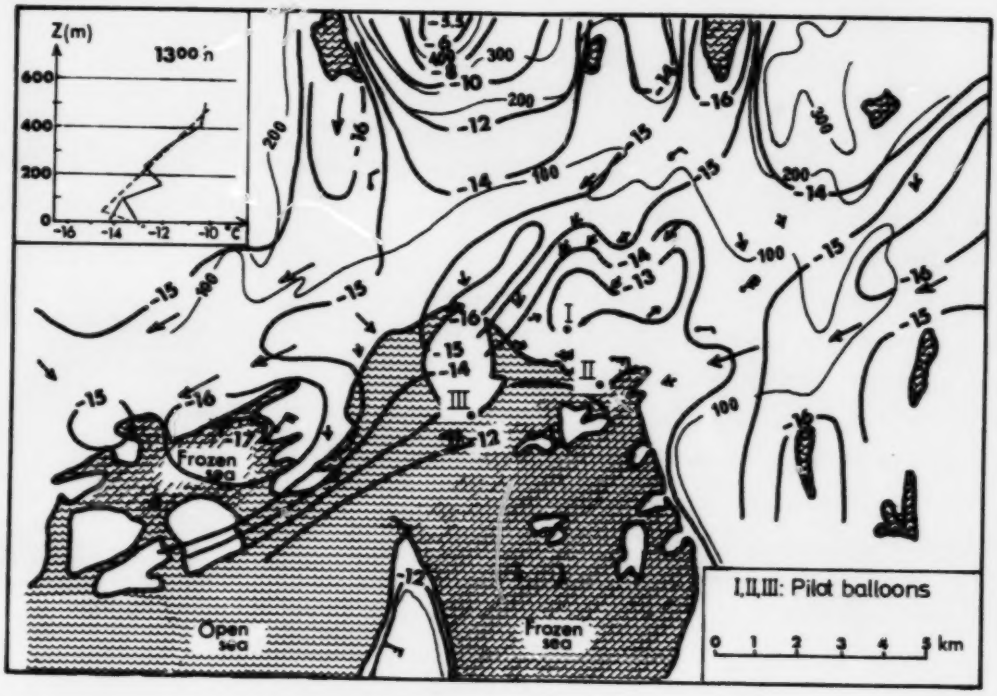

Figure 5.10: The reduced temperature field and the wind field along the ground in Oslo, 6.1.71. 1000h local time.

pressure area was observed over southern Norway, resulting in a weak wind from the west on a synoptic scale.

This appears to be a synoptic situation that typically leads to an inversion situation in the Oslo area. This situation is characterized by weak winds on a synoptic scale. The cloudless sky, which most of the time is necessary to get an inversion, is often observed in the Oslo area during high pressure situations with weak winds from the west.

B. The temperature field

The air temperature was measured near the ground at a great number of locations. A number of cars, equipped with temperature recorders, were employed for this purpose.

All temperature observations were reduced to sea level according to a temperature variation with height of $-1^{\circ}C/100$ m. The reduced temperature field was analysed for the whole region, and the result is given in Figure 5.10.

The air in the upper parts of the valleys is cold and heavy relative to the air over the open fjord and the centre of the city. A force, resulting from gravity, and a pressure gradient caused by the heat sources and sinks in the area, induce local airstreams. The observed wind directions are marked by arrows in Figure 5.10.

C. The variation in temperature with height

In the upper left part of Figure 5.10 the temperature distribution with height is shown. The full line shows the temperatures measured by the thermograph chain placed along the

hillside of Holmenkollåsen. The broken line shows the vertical distribution of the temperature measured by a radiosonde over the centre of the city.

As an example of the temperature variation with height, the results of a series of wiresonde measurements from February 24th are given in Figure 5.11a. In Figure 5.11b the results from the thermograph chain during the same period are shown. The wiresonde measurements show that a neutral to unstable boundary layer existed close to the ground with the thickness of about 100 meter. Between 100 and 150 m, an inversion is observed. Above this layer, the air is more unstable. These main features are also reflected in the thermograph measurements.

If the temperature soundings over the centre of the city are compared with the thermograph recordings, large deviations may occur. This may be due to local effects at the ground stations, and a horizontal variation in the temperature field in the Oslo area.

The temperature soundings show that a considerable heating of a fairly thick layer of air over the centre of the city may occur (see Figure 5.11a).

The thermograph measurements along the hillside may be considered to give only a rough estimate of the temperature stratification and therefore the dispersion conditions over the centre of the city. Two thermograph stations (G, I) in addition to the permanent meteorological stations (A, B, H) should, however, give satisfactory information for the classification of air pollution dispersion conditions. The thermograph placed in the centre of the city gives useful information about the heat island effect.

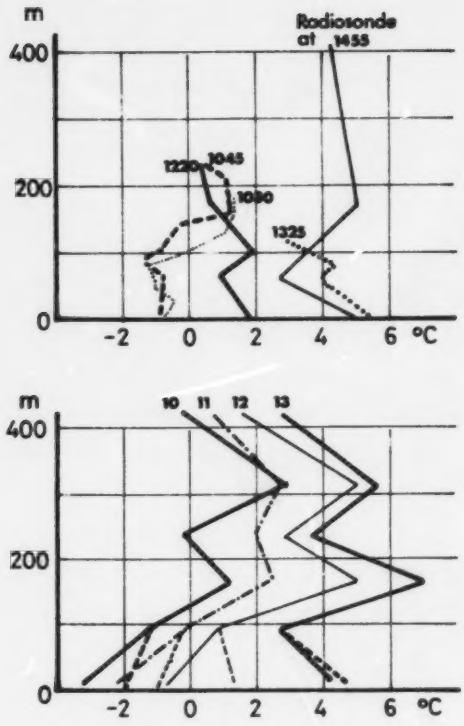

a) Wire- and radiosonde measurements from the centre of Oslo (St. Olavs-plass) between 1030h and 1455h local time.

b) Thermograph measurements at different heights at 10h, 11h, 12h and 13h local time.

Figure 5.11: The temperature distribution with height over Oslo the 24th of February 1971.

D. The wind field

The observed wind directions are marked with arrows in Figure 5.10. On some arrows, barbs indicate the measured wind velocities. A full barb represents 1 m/s, and the short barb 0.5 m/s. As seen from the figure, fairly systematic air streams pass down the valleys towards the relatively warmer areas over the centre of the city and the fjord.

The divergence along the ground was calculated from observed, estimated and interpolated winds in the region. The divergence was mostly negative with maximum values over the centre of the city and over the fjord. Effective heat sources are present in these regions. As a rough approximation, their effect on the wind field was estimated by using as parameters the emission of sulphur from oil combustion and the temperature difference between the air and the open water in the fjord. The sulphur emission was chosen as a parameter believed to be roughly proportional to the heat generating activities.

In addition to the local circulation, a general wind blew through the region from ENE to WSW along the ground, due to the meteorological effects on a larger scale (south eastern Norway).

The vorticity in the region was calculated, but no evident relation was found between this and effects of topography or heat sources.

E. The wind variation with height

The launching sites for the pilot balloons are marked in Figure 5.10 with dots and roman numbers. In Figure 5.12, the horizontal projections of the trajectories are shown. The trajectories show that the local windfield was dominant from the ground and up to a height of 150-200 m. Above this level the larger scale wind field becomes gradually more dominant.

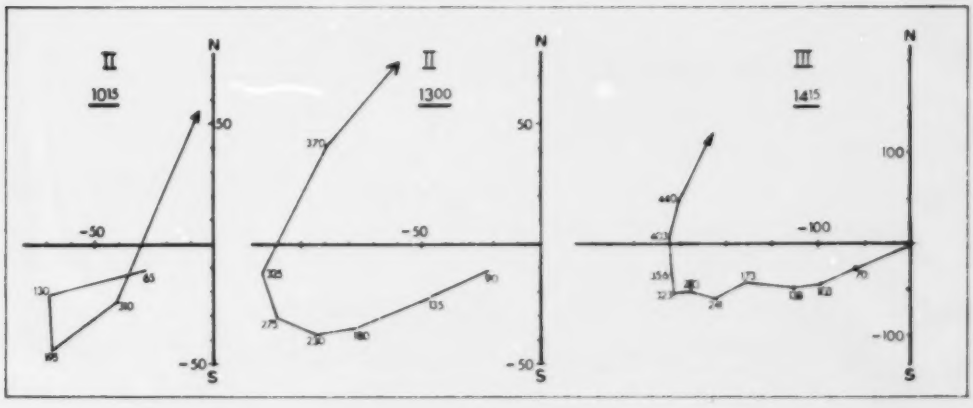

Figure 5.12: Trajectories of pilot balloons relative to their launching sites. The numbers on the curves give the height of the balloon in meter. The roman number indicates the launching site (see Figure 5.10).
Unit: meter.

On the 6th of January, the wind field over Oslo was from the NE while the synoptic wind field was from the SW. This implies that the major change in the wind direction takes place at the height of 200 to 300 m. Both the temperature variation with height and photos of the air pollution show that there are two different wind systems.

In the transition zone, the variation of the wind direction with height is a result of the combined effect of local forces and the frictional coupling with the upper layer.

A change in the wind direction with height of approximately 180° has often been observed during inversion situations. This could indicate a closed circulation within the Oslo basin. On the other hand, the results of time lapse photography did not show any subsidence of the pollution cloud in the surrounding area.

F. A model for the wind field

In order to give the horizontal wind field a mathematical description it is separated in two parts, one divergent part ($\vec{v}_\chi$) and one non-divergent part ($\vec{v}_\Psi$).

$$\vec{v}_h = \vec{v}_\chi + \vec{v}_\Psi; \quad v_\chi = \nabla_h \chi; \quad \vec{v}_\Psi = \vec{k} \times \nabla_h \Psi \qquad \text{(Eq 5.2)}$$

The divergent part is described by a velocity potential χ and the non-divergent part is described by a stream function Ψ. Observed winds at the boundary are used to estimate the stream function along the boundary after correction for the divergent part of the velocity.

A town represents a permanent heat source relative to its surroundings, and will cause vertical motion of the air. As a first approximation the horizontal divergence ($\nabla_h \cdot \vec{v}_h$) is made proportional to the heat sources or some parameter describing the heat sources.

$$\nabla_h \cdot \vec{v}_h = \nabla^2 \chi = a \cdot Q \qquad \text{(Eq 5.3)}$$

Q : heat sources in the region
a : proportionality constant.

The factor of proportionality must be estimated empirically for each region.

The separation of the horizontal wind field into one convergent and one non-convergent part has not yet been properly defined. As a starting point, the velocity potential is defined to be zero along the boundary. It may be shown that in this way, the kinetic energy connected to the convergent part of the velocity is kept at a minimum.

The effect of meteorological processes on a larger scale is taken into consideration by measuring or estimating the wind along the boundary. The measured boundary values are adjusted with respect to the convergent wind field. The remaining part is used to estimate the stream function along the boundary. To estimate the stream function within the region, the following equation is used:

$$\nabla^2 \Psi = 0 \qquad \text{(Eq 5.4)}$$

A method of estimating the vorticity within the region without taking a more complete set of the hydrodynamical equations into consideration has not been found. The intention with the present wind approximation was to calculate the air pollution concentrations within an urban area. It is believed that these concentrations are strongly dependent on the vertical motion of the air, and not very sensitive to small changes in the horizontal wind direction. These wind approximations are better than assuming an homogeneous wind field

in the urban area, specially when the wind field is weak.

The Oslo region was divided into a gridsystem shown in Figure 5.13. The regions with high elevation are excluded from the computations. The network of wind measuring stations in Oslo was adapted to the model studies in this grid system.

The wind fields for the 18th of December 1970 and for the 6th of January 1971 were thoroughly analysed. An estimate of the divergence along the ground showed that this was mostly negative. Further, it seemed to be a reasonable approximation to set the convergence proportional to the emission of SO_2 over the city and to the temperature difference between air and water over the open Oslo-fjord. The empirical form of equation (5.3) for the Oslo area becomes:

$$\nabla \cdot \vec{v}_h = \nabla^2 \chi \quad \begin{cases} a_1 Q_{SO_2} & \text{over the centre of the city.} \\ a_2 (T_A - T_W) & \text{over the open Oslo-fjord, when } (T_A - T_W) < 0. \end{cases} \qquad \text{(Eq 5.5)}$$

Q_{SO_2} : areal sources of SO_2 in the region (given in section 3)

$T_A - T_W$: Temperature difference between air and water

$a_1 = -1.5 \cdot 10^{-5} s^{-1} (\text{ton S}/(\text{km}^2 \cdot 3 \text{ months}))^{-1}$

$a_2 = +3.0 \cdot 10^{-4} s^{-1} \text{deg}^{-1}$

The vertical velocity was calculated from the horizontal divergence by assuming that the three dimentional velocity was non-divergent

$$\frac{\partial w}{\partial z} = - \nabla_h \cdot \vec{v}_h \qquad \text{(Eq 5.6)}$$

The values of a_1 and a_2 are regarded as empirical estimates of the combined effect of gravitational forces and heat sources in the area. It is believed that a_1 and a_2 also are functions of other meteorological parameters within the region (e.g. inversely proportional to the stability of the air). No definite relationship of this kind was found in this investigation.

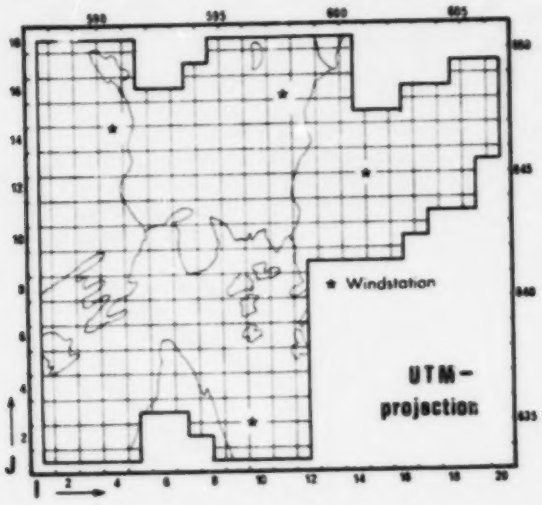

Figure 5.13: The grid system for the Oslo region. The wind recording stations used in the computations are marked by stars.

To estimate the stream function describing the non-divergent wind field in Oslo, the wind measurements from each of the valleys were used. The wind observations were corrected with respect to the convergent wind field, and the corrected measurements from the wind stations M, N, O and P were used to estimate the stream function along the boundary. No air stream was allowed to cross very steep hillsides (for example

along the thermograph chain). The south-western part of the area was used as a compensation zone for the stream function. The computed and measured wind directions in the area were compared in 11 case studies. In the Figures 5.14-17, the arrows (↑) show the calculated wind directions for each grid point. The hached arrows (⬆) show observed wind directions. Some examples will be given below. The observed wind directions are mainly based on the observation of the drifting of smoke from chimneys of height 10 - 20 m above ground level, and on the drifting of soap bubbles about 2 m above the ground. In the lower right part of Figures 5.14-17, the measurements from the thermograph chain are shown.

Date and time of the case studies are given on the individual figures, followed by a short description of the observations and calculations in each of the case studies.

The wind variation with height is often complex during inversion situation and a veering of 180° is often found in Oslo. To indicate the winds on a larger scale the mean velocity measured above the height of 500 m (above the topographic elements) is given in each of the figures. Generally the wind direction changes to the right above this height.

Case study 2: 18th December 1970, 12h (Figure 5.14)

The fjord did not represent a heat source in this case because of the high air temperature. The cooling effect of the fjord would probably be effective only in a shallow layer above the water surface and it is not believed to have

any impact on the general wind field in the area. The vertical temperature stratification was stable (1 deg/100 m) with a neutral part over the city. The area of stagnation coincided with the maximum zone of convergence over the centre of the city.

The main features of the observed and calculated wind fields agreed fairly well. In the area over the fjord, there were discrepancies that might be due to special effects over the fjord not being considered.

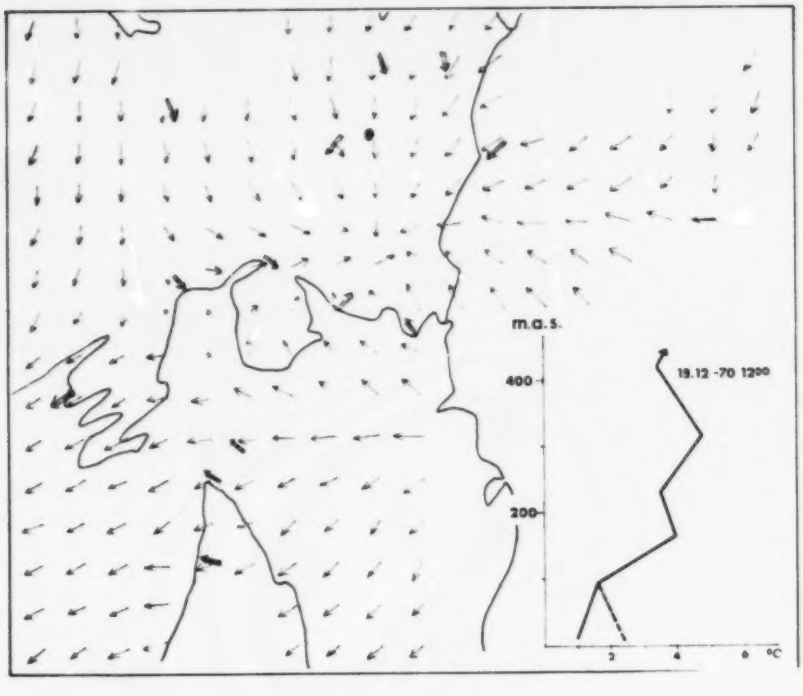

The wind above a height of 500 m: NW 7-8 m/s.

Figure 5.14: Calculated and observed wind directions in case study 2, 18th December, 12h.

Case study 7: 4th February 1971, 12h (Figure 5.15)

The vertical temperature stratification (6 deg/100 m) indicated a very stable air layer in the lowest part of the atmosphere. The air flow in this layer came mainly from the south. No stagnation area was observed over the centre of the city because of the relatively strong wind field. It seemed that the wind station 0 (the computations are based on the observations from this station) has been influenced by a local wind field which may have caused the discrepancies between the computed wind and other wind observations. The observed wind at station B indicated that an air stream from the south was realistic in the northern part too.

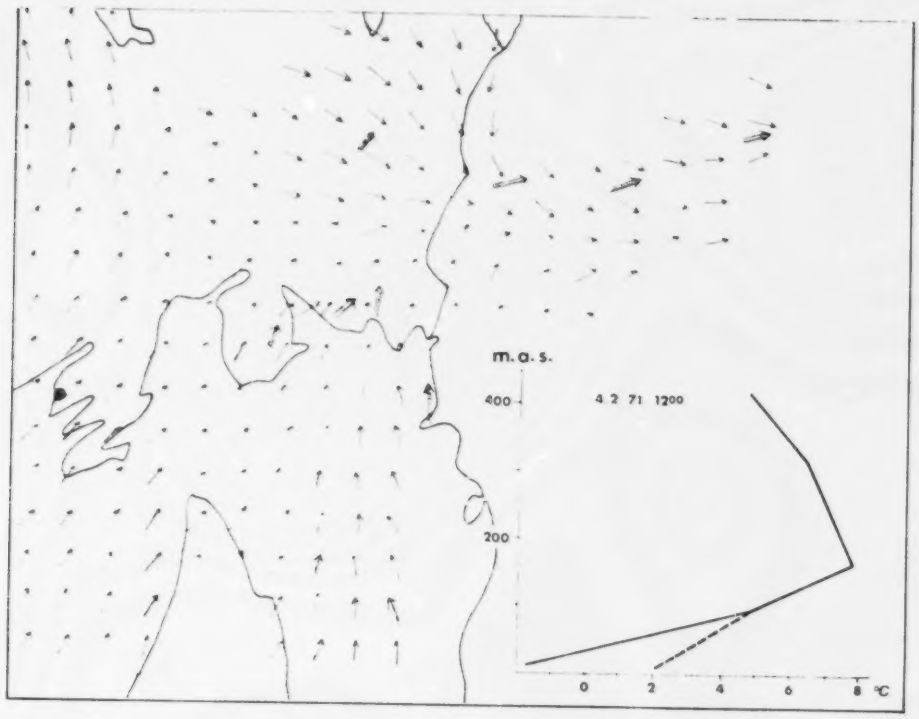

The wind above a height of 500 m: W 10 m/s.

Figure 5.15: Calculated and observed wind directions in case study 7, 4th February 1971, 12h.

Case study 9: 23rd February 1971, 12h (Figure 5.16)

The vertical temperature stratification indicated a moderately stable lower air layer. The general air stream was from the south-west and the stagnation point was moved to the north-east relative to the maximum convergence zone. The calculated and observed wind directions matched well at most points.

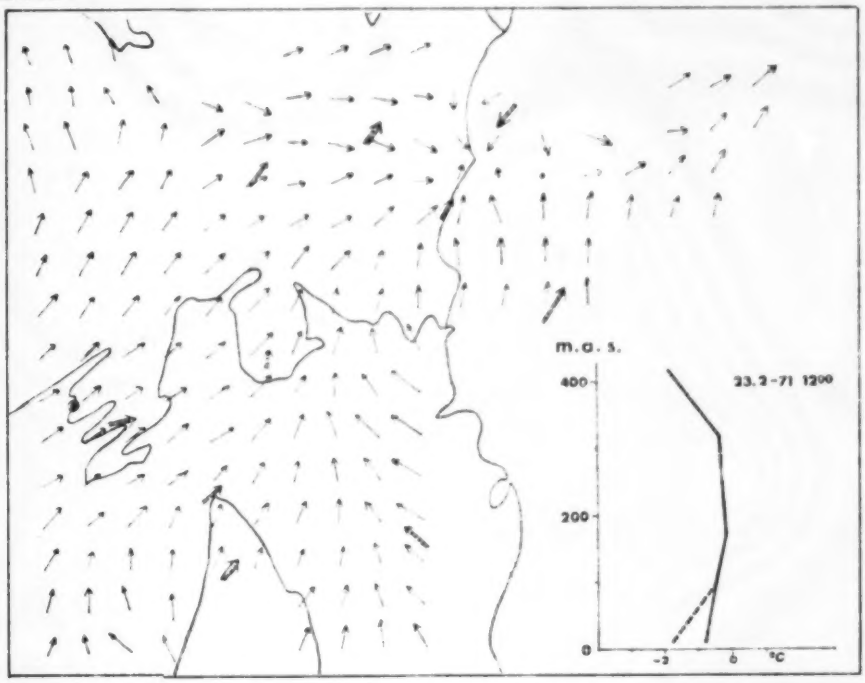

Wind above a height of 500 m: N 3 m/s.
Wind from SW up to 300 m.

Figure 5.16: Calculated and observed wind directions in case study 9, 23rd February 1971, 12h.

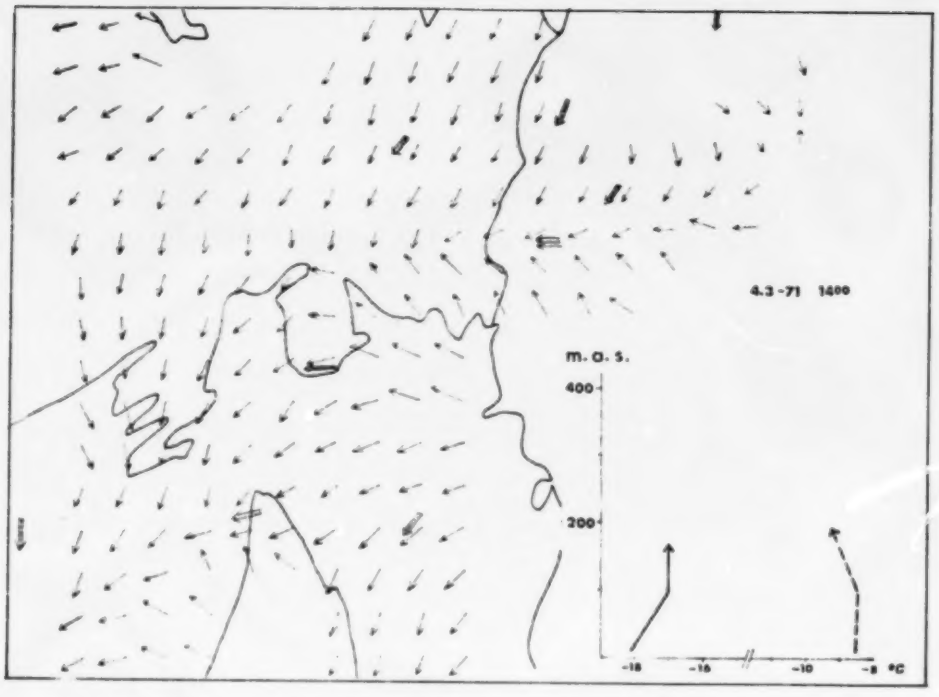

Wind above a height of 500 m: NW 2 m/s.

Figure 5.17: Calculated and observed wind directions in case study 10, 4th March 1971, 14h.

Case study 10: 4th March 1971, 14h (Figure 5.17)

The vertical temperature stratification indicated a moderately stable lower air layer. The general wind came from the north-east and a stagnation point was neither observed nor calculated. The observed and calculated wind directions matched well.

Summary of the case studies in relation to the proposed wind field model

In some case studies the presented wind model did not work well for some regions of Oslo. This may be due to local

canalization of the air flow which is not resolved in the model, or to wind fluctuations which the semi-stationary wind model does not take into account. Besides, the wind model is sensitive to the measurements from the key observation stations in the valleys. Some discrepancies occur because measurements from these stations are not always representative for their region.

The existence of a stagnation point and its location over the urban area of Oslo is reflected in our model calculations. The main features of the air streams around the Oslo-fjord are also reflected in the different case studies. This indicates that the approximation of the convergent wind field works fairly well and that the resulting vertical velocity may be regarded as a first approximation on the scale that is resolved in the grid system.

In order to connect the local wind field to metorological processes on a synoptic scale, processes on an intermediate scale (south-western Scandinavia) has to be considered.

5.5 Concluding remarks

All available wind statistics for the Oslo area show very high frequencies of weak winds, and (as a consequence) the prevailing wind directions vary throughout the area (Figure 5.3). North of the centre the prevailing winds were from the east through north to northwest. In the fjord area the prevailing wind was from the south in the eastern part and from the north in the western part. However, the general picture from the windroses indicates a dominant flow along the directions from the northeast to the southwest. During periods with weak winds, a wind direction towards the centre of the area prevailed on all stations.

The diurnal variation of the wind was significant in the centre of the city, and in the valley north of the centre, whereas the variation in the fjord area was insignificant.

Inversions occurred mostly in the shallow layer below a height of 100-150 m a.s.l. The higher inversions reached most often up to a height of about 300-350 m a.s.l.

A pronounced heat island effect was recorded for the Oslo area, and the effect is closely related to the vertical stability. From the diurnal variation of the regression coefficients in the relation between the heat island effect and the stability, the relative importance of the physical effects involved may be evaluated.

The attempt to calculate the mixing height based on surface temperature observations within and outside the city area and at different heights, showed that the definition was of limited value because it led to a minimum of the mixing height in the middle of the day when the vertical mixing was at a maximum.

Our case studies show that our wind model for the approximation of the convergent wind field in Oslo works fairly well. The location of a stagnation point over the central area and the main features of the air flows over the Oslofjord were well established in the model calculations. In some case studies, however, the presented wind model did not work well, probably due to local canalizations of the air flow which are not resolved in the model, or to wind fluctuations which the semi-stationary wind model does not take into account.

6 RELATION BETWEEN SO_2-CONCENTRATIONS AND METEOROLOGICAL CONDITIONS

6.1 Introduction

This section deals with the relations between monthly, daily and hourly mean values of SO_2 concentrations and meteorological parameters. The monthly and daily mean values are with correction for climatological variations, applied to compare the SO_2 pollution from different years. The hourly mean values are mainly used to investigate the connection between SO_2 concentrations and the meteorological parameters. The statistical investigation was partly made by using all hourly measurements, partly with data from the separate hours of the day, to avoid the diurnal variation in the emission.

6.2 Daily mean values

The trend of the SO_2 pollution was studied by correlating the daily mean values of SO_2 concentrations with meteorological parameters (temperatures and wind observations) from the permanent MI-stations. On the basis of the SO_2 data obtained through the years 1959-63, regression formulas were developed for 10 stations (3). The analysis showed a substantial increase of the correlation by using two instead of one parameter, and an insignificant increase by adding a third parameter. It was common for all stations that the variation on SO_2 concentrations with the temperature difference between station H and B at 19h gave the highest multiple correlation. Below is shown the regression equations for two typical stations 1 and 8. The equations are rewritten to get equations with a stability term and a temperature term. The temperature difference term is assumed to express the ventilation in the Oslo area while the

temperature term is assumed to take care of the variation in the emission of SO_2 due to space heating.

(Eq 6.1) St. 1: $q_{SO_2} = 61.5\ (T_H-T_B)_{19h} - 11.6 T_{B\ 19h} + 472$ $\underline{R = 0.80}$

(Eq 6.2) St. 8: $q_{SO_2} = 47.7\ (T_H-T_B)_{19h} - 1.4 T_{B\ 19h} + 314$ $\underline{R = 0.80}$

q_{SO_2} : SO_2 concentration in $\mu g/m^3$
T : temperature in ^oC
R : multiple correlation coefficient

In the equation for the high elevation station 8 the coefficient of the stability term is more dominating, relative to the coefficient of the temperature term than in the equation for station 1. This difference is probably due to better wind exposure at the high level stations, as inversion strength is negatively correlated with wind speed. The correlation analysis between SO_2 concentrations and single meteorological parameters also indicate that the best single meteorological parameter correlated with the SO_2 concentrations is the wind speed for the high level stations, and the temperature for the low level stations.

These regression equations are applied to estimate the real change of the SO_2 pollution from the years 1959-63 to 1970 and 1971. In Figure 6.1 the relation between observed concentrations and concentrations calculated by means of the regression equation for station 1 is shown. The regression equation is based on the data from the period 1959-63. The points representing the years 1959-63 must necessarily be equally distributed around a 45^o-line. All the points representing 1970 (January and February) and the points representing 1971 (January, February and March) are

below the 45°-line. This means that the concentrations observed in the last two years are significantly lower than should be expected if the emission conditions for the SO_2 were unchanged since 1963, with respect to the amount of sulphur, emission heights and the number of sources near the measuring point.

The investigations indicated that the SO_2 pollution has been reduced with 50 to 60% since 1965. According to information from the oil companies the SO_2 emission has been reduced with approximately 40% in the same period (see section 3). The difference may be ascribed to more sentralized heating systems and greater emission heights in the last years.

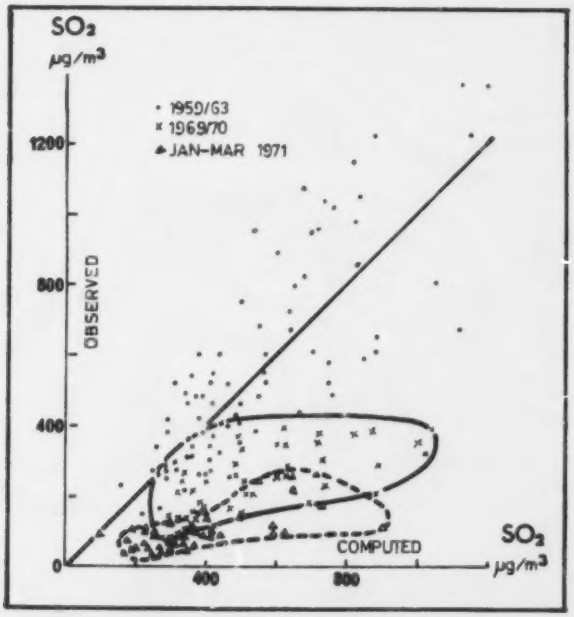

Figure 6.1: Relations between observed and computed values of SO_2:

$$q_{SO_2} = 61.5\ (T_H - T_B)_{19h} - 11.6 T_{B19h} + 472.$$

6.3 Monthly mean values

In Figure 6.2 is shown the variation of the mean concentrations of SO_2 and suspended particulates for the 2-10th week through the years 1959-63, 1970 (station 1) and for 1971. The mean concentrations the last two years are low compared with the previous years. The variation in first half of the sixties was, however, great due to climatological variations. It is also seen that the variations at all stations were similar.

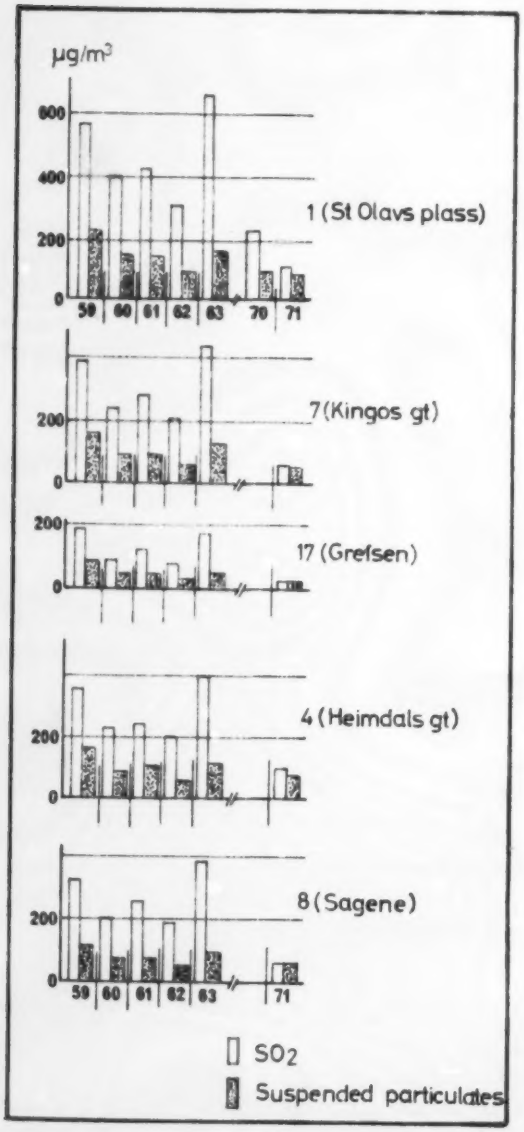

Figure 6.2:
Mean values of SO_2 and suspended particulates at 5 stations from 1959 to 1971, 2-10th week.

Since the regression analysis showed a close connection between the daily mean SO_2 concentrations and the temperature difference between the meteorological station H and B (the vertical temperature stratification), the number of inversion situations was chosen as a climatological parameter in order to compare mean SO_2 concentrations from year to year.

In Figure 6.3 the monthly mean values of SO_2 (station 1) and the corresponding mean frequencies of inversions for the winters 1959-65 were compared with the winters 1969/70 and 1970/71. For 1970/71 the inversion frequencies in November and March were equal to mean frequencies for the same months in the years 1958-64. The mean temperatures for the months November and March 1970/71 were respectively 2.2 and 2.0°C lower than the mean temperatures for the same months in the period 1958-64. The mean SO_2 concentrations for 1970/71 were 30-40% of the respective mean concentrations for the years 1958-64. Other winter months such as December 1969 may be compared in the same way with earlier years, showing about the same reduction in percent. The mean temperature in December 1969 was 0.7°C lower than i 1958-64.

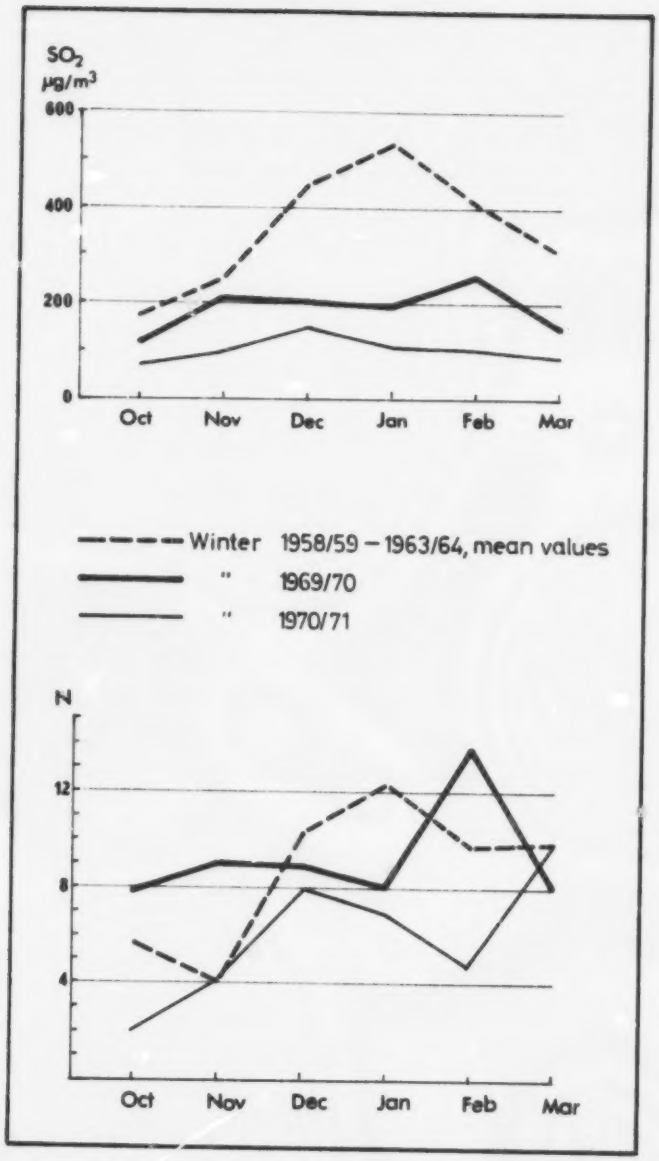

Figure 6.3a:
Monthly mean values of SO_2 at station 1 for the winters 1958/59 - 63/64, 1969/70 and 1970/71.

Figure 6.3b:
Monthly frequencies of inversions in Oslo for the winters 1958/59 - 63/64, 1969/70 and 1970/71.
N= inversion frequency given as number of days with higher temperature at 07h at station H than at station B.

In Figure 6.4 the variation of the SO_2 concentrations is shown for the two periods (2-10th week) of 1960 and 1970 with comparable frequencies of inversion and mean temperatures. The mean concentrations in the centre of the city was in 1970 reduced to approximately the half of the concentrations in 1960. This is in accordance with the results shown in the previous paragraph.

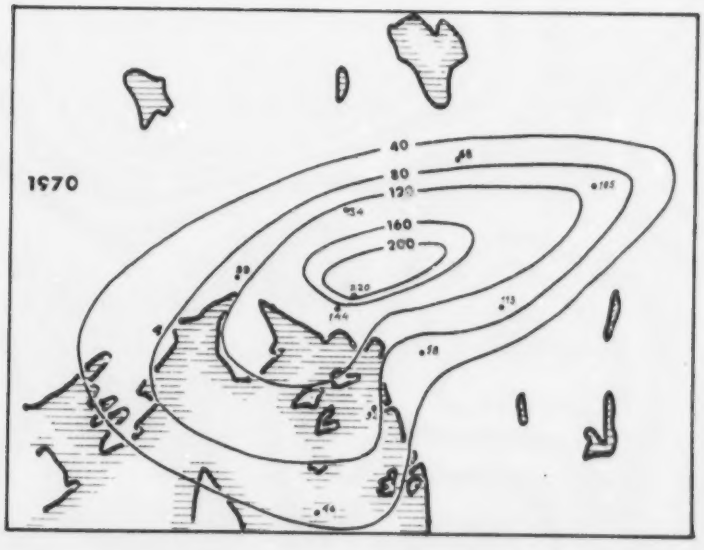

Figure 6.4: The spatial variation in Oslo of SO_2 concentrations ($\mu g/m^3$) in 1960 and 1970, 2-10th week.

6.4 Hourly mean values

A. Relation between SO_2 concentrations, wind and stability

Figure 6.5 shows the total SO_2 pollution roses for station 26 in the centre of the city and one station southwest of the centre (station 31), based on the wind data from station L for every 10° wind sector. The wind rose for the other city wind station K is similar. Due to better data coverage the wind station L was chosen for the presentation. These pollution roses are generally expected to point out the important pollution sources in the area (see section 4). The presented roses are very similar and indicate a great area source located towards east-northeast of station 31 and east of station 26. The pollution rose for station 26 indicates SO_2 pollution with winds from all directions, which is typical for a station situated within a great area source. Station 31 had lower mean values, due to the more periphere position relative to the city centre. With winds from east to northeast, the mean concentrations at station 31 was highest relative to station 26 (St. Olavsplass). This occurs mainly during the night and the morning hours (compare also with Figure 4.5).

Figure 6.6 shows the SO_2 pollution roses for simultaneous measurements at station 26 and 30, the latter situated in the northern part of the centre and at an altitude of 80 m a.s.l. The wind observations from the northern part of Oslo (station 0), were used for the wind classification.

The difference in the pollution roses for station 26 in Figures 6.5 and 6.6 may partly be due to nonidentical data series, but also to the different wind regimes of the two wind measuring stations employed. A comparison of the pollution roses for station 26 shows that interpretation of pollution roses with respect to directions to source regions must be made with great care.

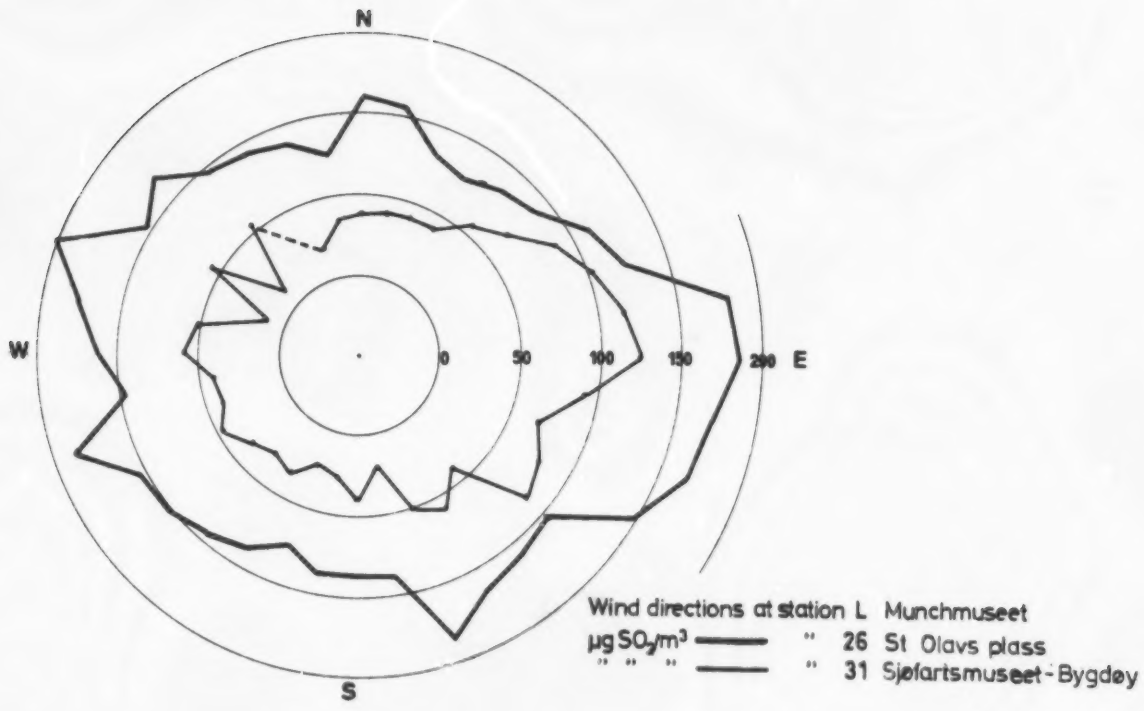

Figure 6.5: SO_2 pollution roses for stations 26 and 31. Mean concentrations of SO_2 from December through February 70/71 at stations 26 and 31 for all wind directions observed at wind station L. Hourly observations and all stability classes are used. Unit: µg SO_2/m^3.

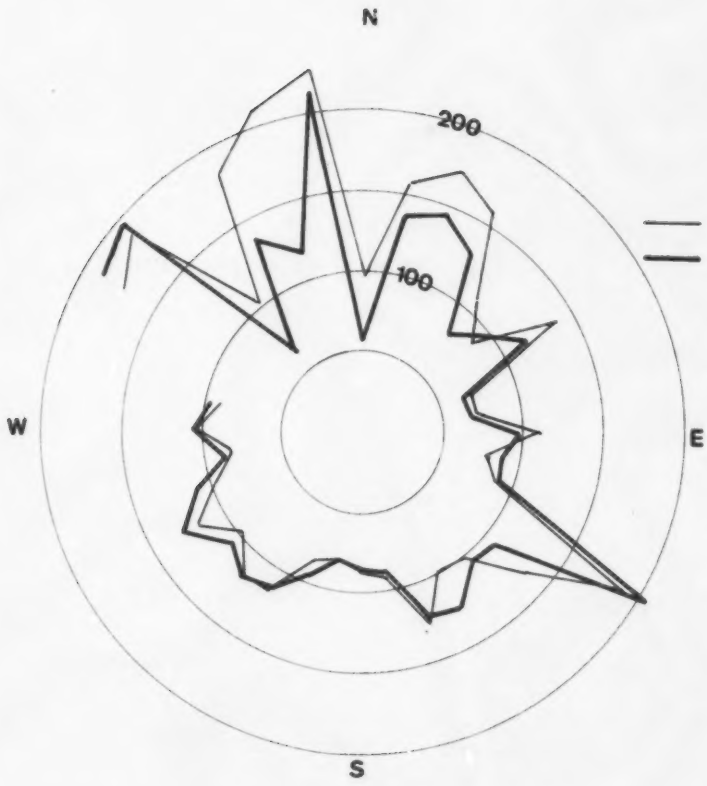

Figure 6.6:
SO_2 pollution roses for stations 26 and 30. Mean concentrations of SO_2 for December through February 70/71 for all wind directions observed at wind station 0. All stability classes. Hourly observations.
Unit: µg SO_2/m^3.

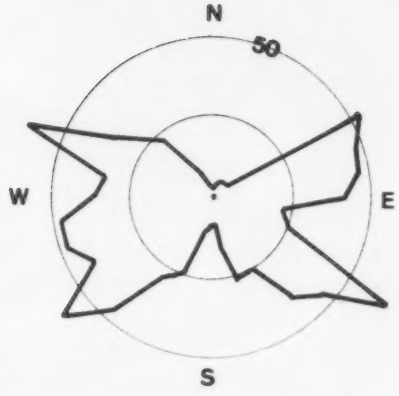

Figure 6.7: SO_2 pollution rose for station 27 (Vollebekk) for December through February 70/71 based on wind observations from station N (Valle Hovin). All stability classes. Hourly observations.
Unit: µg SO_2/m^3.

The mean SO_2 concentrations arising from a southerly wind direction were nearly equal on the two stations in Figure 6.6. Station 30 had slightly larger concentrations, indicating different accumulation lengths of pollution for the two stations. The difference in elevation did not seem to have any effect on the concentrations of SO_2.

The different accumulation lengths in the area source could contribute to the great differences of the mean SO_2 values due to the typical wind direction from north at station 0 during pollution episodes. In addition, the vertical mixing may also be reduced with northerly winds which most frequently occur during the nighttime (see 5.3A and Figure 4.5). The study of pollution roses for different wind speeds and stability conditions shows that with wind speeds below 2 m/s the SO_2 concentrations were generally highest at the high level station (30). With wind speed higher than 2 m/s the mean SO_2 concentrations were highest at the low elevation station (26), probably due to the different wind exposure at the two SO_2 stations. Different stability-classes did not appear to influence the dependence of SO_2 concentrations on wind direction. This indicates that emissions close to the ground are dominant in Oslo.

The pollution rose for station 27, located in the suburb of Oslo, is shown in Figure 6.7. The mean SO_2 concentrations indicate an area source towards west and two distinct point sources in easterly directions.

B. Multiple regression between hourly mean values of SO_2 and temperatures

A multiple regression analysis similar to the one mentioned in paragraph 6.2 was applied to hourly mean values of SO_2 at station 26 in the centre of Oslo and hourly mean temperatures and wind velocities. This study may also serve as a test of the method employed to estimate the reduction of the SO_2 pollution in the last ten years by means of the regression analysis of the daily SO_2 concentrations. In this study, all NILU thermograph stations were used in addition to the permanent MI-stations.

First all hourly SO_2 concentrations were correlated with temperatures and wind velocities. The correlations between SO_2 concentrations and each single parameter were low. The best single parameter turned out to be temperature from the low elevation stations A (R=0.38) and C (R=0.36). Wind velocities were poorly correlated with hourly SO_2 concentrations. The best wind stations to describe the SO_2 concentration turned out to be O (R=0.16) and N (R=0.15). This means that a single wind velocity is not sufficient to describe the air ventilation in the Oslo basin.

Like for daily mean values, the correlation coefficients showed a substantial increase by introducing two temperatures. The two temperatures being highest correlated with the SO_2 concentrations at station 26 were:

$$q_{SO_2} = -26.8\ T_B + 24.5\ T_F + 143 \quad \text{(Eq 6.3)}$$

q_{SO_2} : The hourly SO_2 concentration in $\mu g/m^3$

T_B : temperature at station B (96 m a.s.l.)

T_F : temperature at station F (317 m a.s.l.)

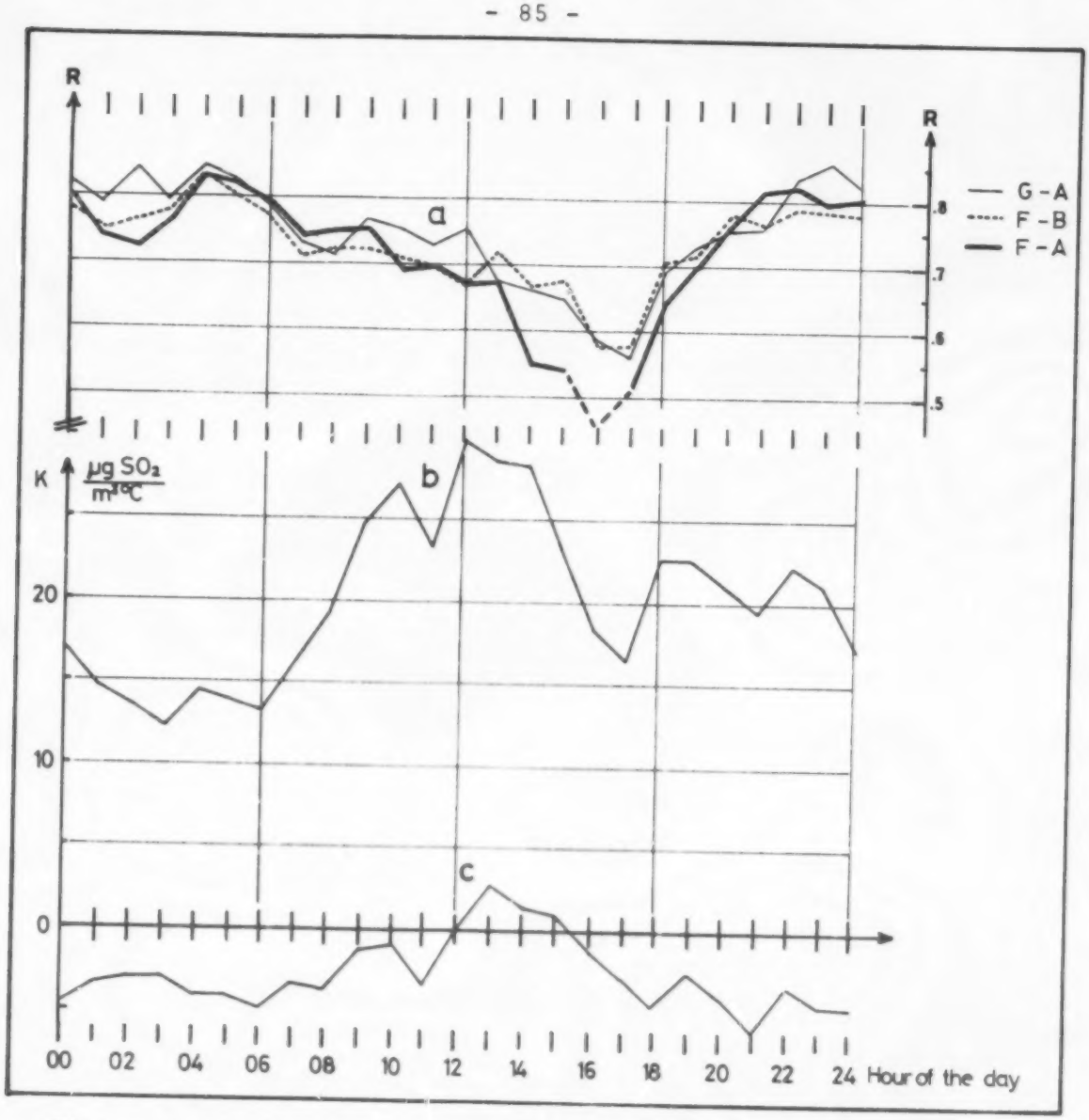

Figure 6.8: Diurnal variations of

a) the multiple correlation coefficients (R) between hourly mean SO_2 concentrations (q_{SO_2}) and the temperature differences for the station pairs G-A, F-B, F-A.

b) the stability factor k_1 in the regression equation between q_{SO_2} and the temperature differences for the station pair G-A (see Eq 6.4).

c) the temperature factor $k_1 + k_2$ in the same equation (see Eq 6.4).

To avoid the effect of the diurnal differences in emission, when comparing the hourly SO_2 concentrations with meteorological conditions, the analysis was performed separately for each hour of the day. Temperature difference was best correlated with the SO_2 concentrations in all hourly regression analysis.

The diurnal variation of this relationship was studied for station 26 in the centre of the city. The diurnal variations in the correlation coefficients for the highest correlated temperature differences are given in Figure 6.8a. The correlation coefficients showed diurnal variations with generally a maximum at night and a minimum in the afternoon. During the night about 60% of the SO_2 variance and during daytime only about 30% of the variance may be explained by two temperatures measured simultaneously at different heights. The temperature difference between stations A and G generally showed the best correlation with the hourly SO_2 concentrations.

By rewriting the regression equations,
from $q_{SO_2} = K_1T_1 + K_2T_2 + K_3$

to $q_{SO_2} = K_1(T_1 - T_2) + (K_1 + K_2)T_2 + K_3$ (Eq 6.4)

further information may be extracted by studying the diurnal variation of the coefficients K_1 and K_2. Figure 6.8b and 6.8c show the variation in K_1 and $K_1 + K_2$ respectively for the station pair A and G. The other station pairs show similar variations. The stability term $K_1(T_1 - T_2)$ is the most important term in this relation (Figure 6.8b), as the correlation between q_{SO_2} and $(T_1 - T_2)$ was in general only slightly lower than the multiple correlation in the regression equation $q_{SO_2} = K_1T_1 + K_2T_2 + K_3$.

The diurnal variation of the coefficient in the stability term (curve b) shows a maximum at daytime. This may to some extent be due to the effect of the diurnal variations of the ventilation. On the other hand, the diurnal variation of the vertical mixing of the air should imply a maximum of the coefficient at night. The variation of the coefficient of the stability term is fairly similar to the diurnal variation of the space heating. It is therefore believed that the diurnal variation of this constant is mainly determined by the diurnal variation in emission. This relation may therefore be applied to quantify the effect of variation in the general emission conditions on the ambient air concentration of SO_2 in Oslo. This is shown in Figure 6.1.

On the other hand, the constant in the temperature term which is generally expected to be best related to space heating (negatively correlated with q_{SO_2}), becomes positive in the middle of the day (see Figure 6.8c). As mentioned above (see paragraph 4.3 p.30) local effects due to sun radiation at daytime may be important for the interpretation of the SO_2 variation. The radiation generally results in a temperature rise which is accompanied by stagnation of the air and a maximum of pollution concentrations. This may explain the positive temperature term at daytime.

C. Relation between SO_2-concentrations and different combinations of meteorological parameters

To examine further the connection between the SO_2 concentrations and meteorological parameters, different combinations of the original observations were evaluated in the regression analysis.

Instead of employing the wind velocity at the different stations, a ventilation parameter was defined as the product of the velocity component towards the centre of the city at the stations O and N and the cross section of the respective valleys. The correlation coefficient between this parameter and the hourly SO_2 concentrations in the city (R=0.3-0.5). was higher than the correlation with single wind velocities, but still the correlation with vertical temperature gradient was superior.

The connection between the SO_2 concentrations and the mixing height, as defined in paragraph 5.3D, was examined, but did not show any better correlation than the temperature differences (R=0 - 0.35). This means that the mixing height did not describe the vertical mixing or flux of SO_2.

The relative humidity shows a negative correlation with the hourly SO_2 concentration, with correlation coefficient from 0.2 to 0.3 and a maximum of the correlation in the morning.

6.5 The investigation of particulate sulphur as air pollution in Oslo

The filters from six of the SO_2 measuring stations in Oslo (stations 2, 3, 4, 6, 7 and 11) were analysed with respect to the sulphur content and the content was transformed into daily mean values of air concentrations.

The mean values and their standard deviation are given in Figure 6.9. Multiple linear regression analyses were performed to clarify the connection between particulate sulphur and different meteorological parameters like temperature, wind, relative and absolute humidity, and different pollution measurements like suspended particulates and SO_2 concentrations. A linear combination of temperature, humidity and SO_2-concentration described 60-80% of the variance of the particular sulphur content of the air.

A closer investigation of the relation between the particulate sulphur content and several products of the parameters listed above was performed. For all the stations involved in the investigation, it turned out that the variation in the particulate sulphur content was best described by the product of the SO_2 concentration and relative humidity, and that this product was better than a linear combination of the two parameters.

It may be assumed that the oxidation of SO_2 is the main source of particulate sulphur in an urban area. The residence time for the air in the Oslo region is important for the relation between the particulate sulphur content and the SO_2 concentration. A long residence time will result in high SO_2 concentrations and an increased part of SO_2 will be oxidized to particulate sulphur.

The dependence on relative humidity indicates that the oxidation process is intensified with increasing (relative) humidity, which is reasonable from a chemical viewpoint.

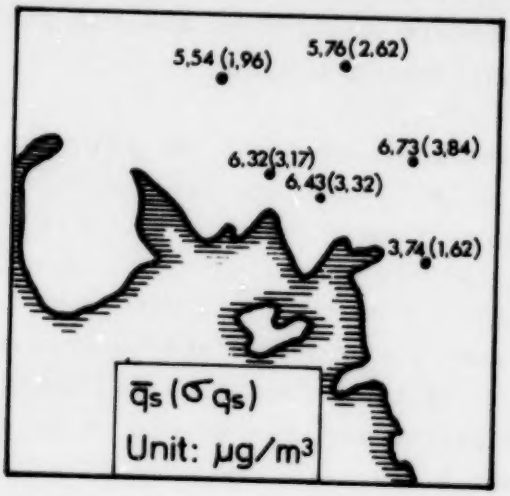

Figure 6.9: The mean ambient air concentrations of particulate sulphur in pollution situations. The standard deviation is given in brackets.

With a SO_2 concentration of 200 µg/m³ and an increase in relative humidity from 80 to 90%, the particulate sulphur that was collected by the filter increased by 1.7 µg S/m³. A quantitative estimate of the increased oxidation rate with humidity showed that the residence time of the air was an important parameter. This effect may effectively be studied in model calculations.

Since the particulate sulphur concentrations were small, they will have very little effect on the SO_2 concentrations.

6.6 Concluding remarks

The two studies of the trend of the SO_2 pollution from the years 1958-65 to 1970/71 by means of daily and monthly mean values of SO_2 respectively led to similar results, although different methods were applied to correct for the meteorological variations from winter to winter. The SO_2 pollution has been reduced by about 50-60% from 1965 to the winter 1970/71, which agrees fairly well with the calculated reductions in SO_2 emissions and the change of the emission heights. The pollution of suspended particulates was in the same period reduced by roughly 30%.

Both for daily and hourly mean values, it was shown that the variation of the SO_2 concentrations was best described by means of a stability parameter (temperature difference between two levels) rather than wind parameter and a definition of mixing height. The study of the diurnal variation of the coefficients in the regression equation between hourly mean values of SO_2, temperature and temperature variation with height (stability) indicated that the diurnal variations in the coefficient of the stability term and the emission were similar. The coefficient of the temperature term also varied in a similar way (positive maximum in the middle of the day), and as a consequence, the temperature term may not be considered as a heating term when hourly values of SO_2 are considered.

The pollution roses indicate that the central Oslo area may be characterized as a large area source. A comparison between SO_2 measurements at different heights indicates good mixing up to approximately 100 m a.s.l.

The regression analysis has established a close relation between particulate sulphur on the filters, the SO_2 concentration and relative humidity of the air. This connection may be used to estimate the oxidation rate of SO_2 in Oslo if the residence time of the air masses and the emission of SO_2 is known.

7 THE AIR POLLUTION MODEL FOR OSLO

7.1 Introduction

To establish the connection between the emissions of SO_2, the weather conditions and the SO_2 concentrations in the ambient air, it was found necessary to study short term variation in the SO_2 concentrations, representative for the Oslo area.

In many applied models, a Gaussian diffution formula is used to estimate the dispersion from a large number of single point sources or groups of point sources within an urban area (18) (19). A Gaussian diffusion formulae is known to describe well the dilution of pollutants under certain simplified wind conditions. These wind approximations are not realistic in Oslo (see section 5).

The pollution concentrations in an urban area depends on both meteorological and chemical processes within the air masses above the area. Emission of pollutants is often associated with emission of heat. In that way, both the "chemical" and meteorological conditions are changed due to the emission. The extrapolation of measurements of the ambient air concentration to other conditions of emission is difficult without knowing the importance of the different processes that cause these changes.

In a comprehensive system approach to abatement strategy, the connection between a reduction in emission and the corresponding change in ambient air concentrations is approximated by a linear relationship (20). The air quality standards are set according to biological effects that primarily depend on the concentration near the ground. When a local problem is

considered, it is the ground level concentrations that have to be considered. On a larger scale, the total emission has to be considered together with the cleaning processes of the atmosphere.

In the city of Oslo, a local air pollution problem is studied. The horizontal transport of pollution will not carry the pollutants away from the ground level although they will be diluted. Systematic vertical motion will transport the pollutants away from the ground level more rapidly. Therefore, it is important to estimate the relative importance of these two transport components.

It is rather difficult to analyse the chemical processes that result in a transformation of the pollution components. As a first approximation, one has assumed a sink of SO_2 in the Oslo air to be dependent on the SO_2 concentration alone.

H. Reiquam was the first to perform model-calculations for the Oslo airshed (4). His calculations showed that the use of a finite grid system (a box model) might be useful in Oslo. One might say that his work has been continued in the model studies during the winters of 1969/70 and 1970/71. A preliminary model, (as a numerical solution of the continuity equation for SO_2) was developed and tested after the first winter (21). A stream-function was used to describe the horizontal wind field, and a sink term was made proportional to the concentration. The vertical flux of SO_2 was incorporated in this term as a first approximation, and the factor of proportionality was made dependent on the vertical temperature stratification. The value of this factor was chosen in order to match the observed and calculated concentrations. The factor had to be given a very high value which indicated that systematic vertical motions

are important as a transport component. This conclusion was supported by detailed wind observations in a number of case studies (see section 5.4).

7.2 Mathematical description

As a mathematical frame for the model studies, the continuity equation for the pollution component (eq. 7.1) was used.

$$\text{(Eq. 7.1)}\quad \frac{\partial q}{\partial t} = -\nabla_h \cdot (\vec{v}_h q) - \frac{\partial}{\partial z}(wq) + \nabla_h \cdot (K_h \nabla_h q) + \frac{\partial}{\partial z}\left(K_z \frac{\partial q}{\partial z}\right) + \text{sources} + \text{sinks}$$

t	: time
x, y, z	: orthogonal coordinates with unit vectors, $\vec{i}, \vec{j}, \vec{k}$.
q	: pollutant concentration
K_h, K_z	: horizontal and vertical diffusion coefficents
$\vec{v}_H = u\vec{i} + v\vec{j}$	: horizontal velocity
$\nabla_h = \vec{i}\frac{\partial}{\partial x} + \vec{j}\frac{\partial}{\partial y}$	: horizontal gradient operator
w	: vertical velocity

In an urban area, there exists a lot of small sources at different elevations up to a certain height H. Within this area the buildings and the heat sources at different elevation lead to enhanced turbulence and mixing of the air. In the computations, the mean concentration in this lowest part of the atmosphere is considered. It is very difficult to consider each single source and the equation is integrated vertically:

$$\text{(Eq. 7.2)}\quad \frac{\partial \bar{q}}{\partial t} = -\overline{\nabla_h \cdot (\vec{v}_h q)} - \frac{(wq)_H}{H} + \overline{\nabla_h \cdot (K_h \nabla_h q)} + \left(\frac{K_z}{H}\frac{\partial q}{\partial z}\right)_H + \overline{\text{sources}} + \overline{\text{sinks}}$$

$(\bar{\ })$: the mean value in the lowest part of the atmosphere with height H.

As a finite difference approximation of Eq. 7.2, a forward time step and an upwind finite difference system were used.

The finite difference approximation introduces a large artificial diffusion. Estimates of the actual diffusion coefficients show that the horizontal diffusion term in Eq. 7.2 is small compared with the artificial diffution on a km scale. Therefore, the horizontal diffusion terms are left out of the computations. The vertical diffusion term is regarded to be small in inversion situations and as a first approximation it is most convenient to leave it out of the computations.

The threedimensional wind field was calculated from the wind measurements by the presented wind model (see section 5.3F). Forward differences in time combined with upwind differences in space seem to be appropriate for Eq. 7.2 if slow fluctuations in the concentration are considered. In an urban area, these often are the more important. A relatively large artificial diffusion is built into the finite difference form. On the other hand, this form is simple, stable and ensures mass consistence.

The finite difference form of Eq. 7.2 was solved as an initial value problem in the grid system shown in Figure 5.13. The sources of SO_2 are quantified from the results of the emission survey presented in section 3. The spatial distribution given in Figure 3.3 was used with the Eq. 3.1 to calculate the hourly emission of SO_2 in the area ($Q_{SO_2}(T_i,t_h)$.

The sink term of SO_2 (A) was assumed to be a function of the SO_2 concentration in the following way:

$$A = cq + dq^2 \qquad \text{(Eq. 7.3)}$$
$$c = 1.0 \cdot 10^{-6} s^{-1}$$
$$d = 0.25\ s^{-1}\ (g/m^3)^{-1}$$

The functional form of A and the values c and d are estimated by J. Nordø in connection with modelling long range transport of air pollutants (22).

The dependence of the particulate sulphur content of the air on the relative humidity, discussed in section 6.5, indicates that this should be taken into consideration in the sink term. However, the relative humidity is not expected to have a great influence on the SO_2 concentration. The three-dimentional wind field was calculated from meteorological observations from hour to hour by the wind model presented in section 5.4F.

7.3 Results

The wind model was used together with the presented estimates for the sources and sinks for SO_2 in the region, and the SO_2 concentration was calculated for all the grid points for the 4 days: 17th-18th of December 1970, 3rd-4th of January 1971, 4th-5th of January 1971 and 5th-6th of January 1971.

The timing of the daily measurements was the reason for choosing the calculation interval to be 24 hours from 14h local time. The initial value of the SO_2 concentration was set at zero. This approximation has a small influence on the calculated concentration during the first few hours. There was not found any reason to improve this approximation although this could easily be done, by using

for example the steady state solution for the given wind field as an initial value.

The upwind boundary value for the SO_2 concentration was set to zero all the time. At the downwind side of the area, the finite difference approximation did not demand any artificially set boundary value, as the pollution was brought out of the region with the air movement.

The hourly mean SO_2 concentrations at four stations were compared with the calculated values at the grid points within the same kilometer squares.

Two of the stations, 26 and 30 were located in the centre of the city (Figure 4.1). The difference in height between these stations was about 70 m. The SO_2 measurements (see section 6.4A) indicate that the difference in elevation of the two stations did not in itself result in different concentrations. This supports our assumption of mixing in the lowest layer. The two other stations were placed to the south (31) and north (28) of the city centre.

Figure 7.1 shows the calculated and observed values at the four stations for the period from 15h on the 17th of December to 14h on the 18th of December. During the night, the windspeed slowed down from about 5 meter per second to an irregular wind of about 1 meter per second. This is the reason for the increase of the SO_2 concentration that is observed and calculated.

The calculated increase at St. Olavsplass is lower than the observed increase. It is possible that an investigation of such discrepancies might be used to improve the model. In this case the calculated values are too much influenced by

the clean air over the fjord. An increase from about 100 µg SO_2/m^3 to about 300 µg SO_2/m^3 at St. Hanshaugen and an increase from about 30 µg SO_2/m^3 to 100 µg SO_2/m^3 at Bygdøy compared well. The calculations at Kjelsås did not show large change, and the measurements did not show any fluctuation at all. The reason for this may be the limited sensitivity of the instrument used.

From the presented calculations, it may be concluded that the response of the SO_2 concentration on larger changes in wind velocity was correct with respect to time and space. This indicates that the emission of SO_2 and the wind field are taken into consideration as a fair approximation.

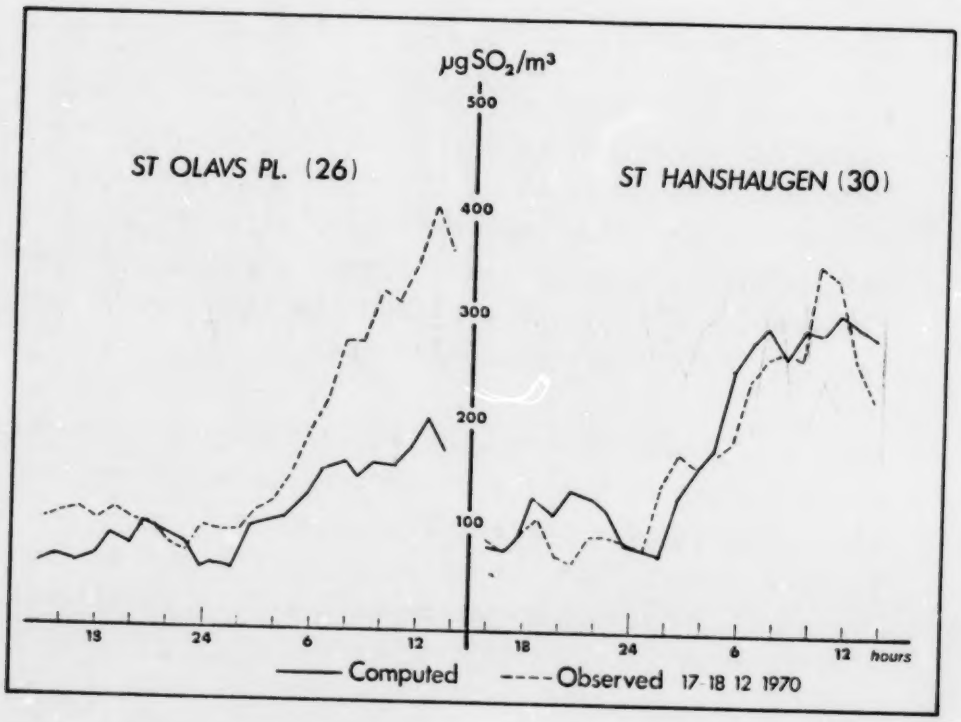

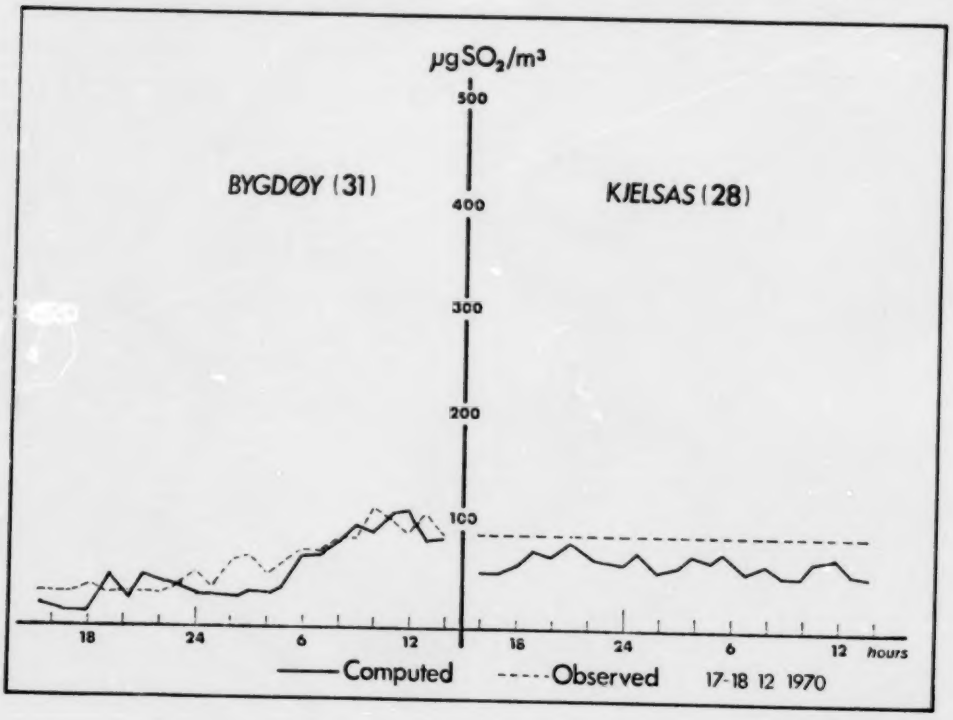

Figure 7.1: Computed and observed SO_2 concentrations.

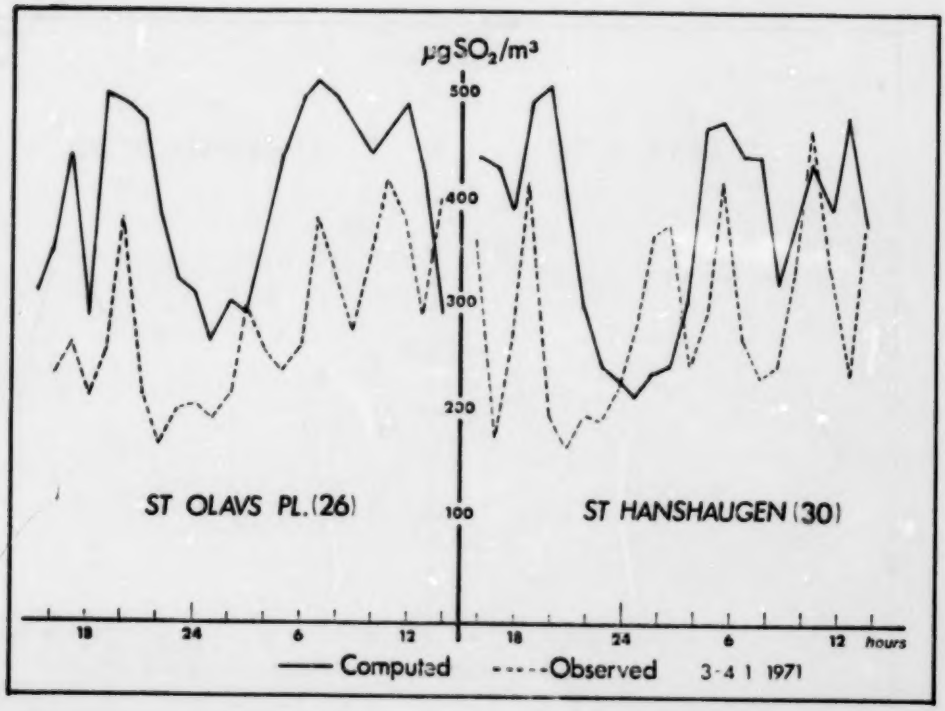

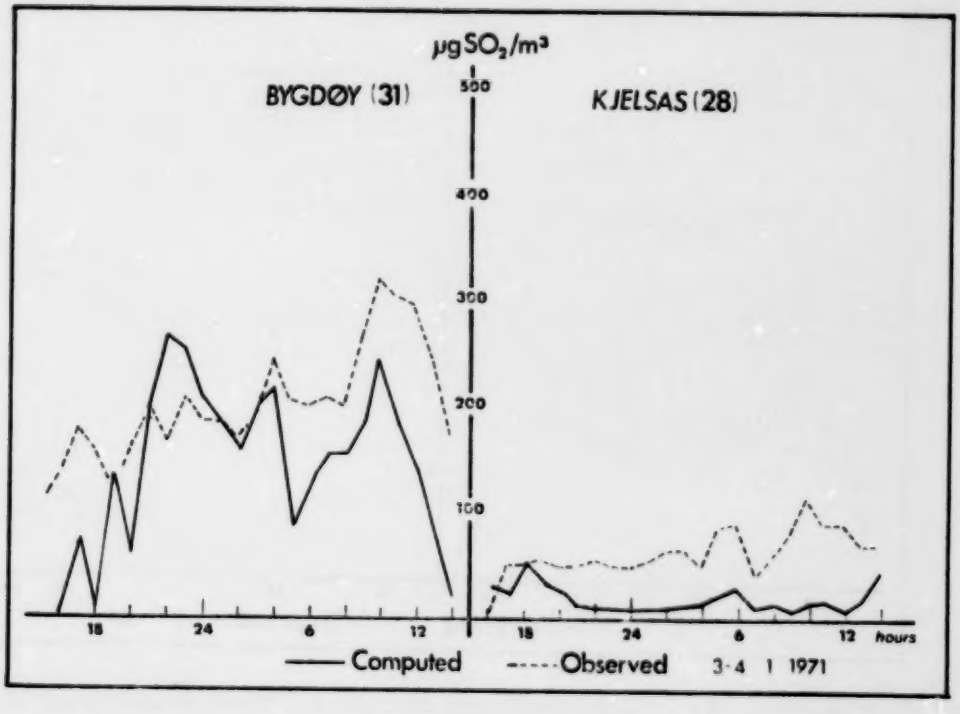

Figure 7.2: Computed and observed SO_2 concentrations.

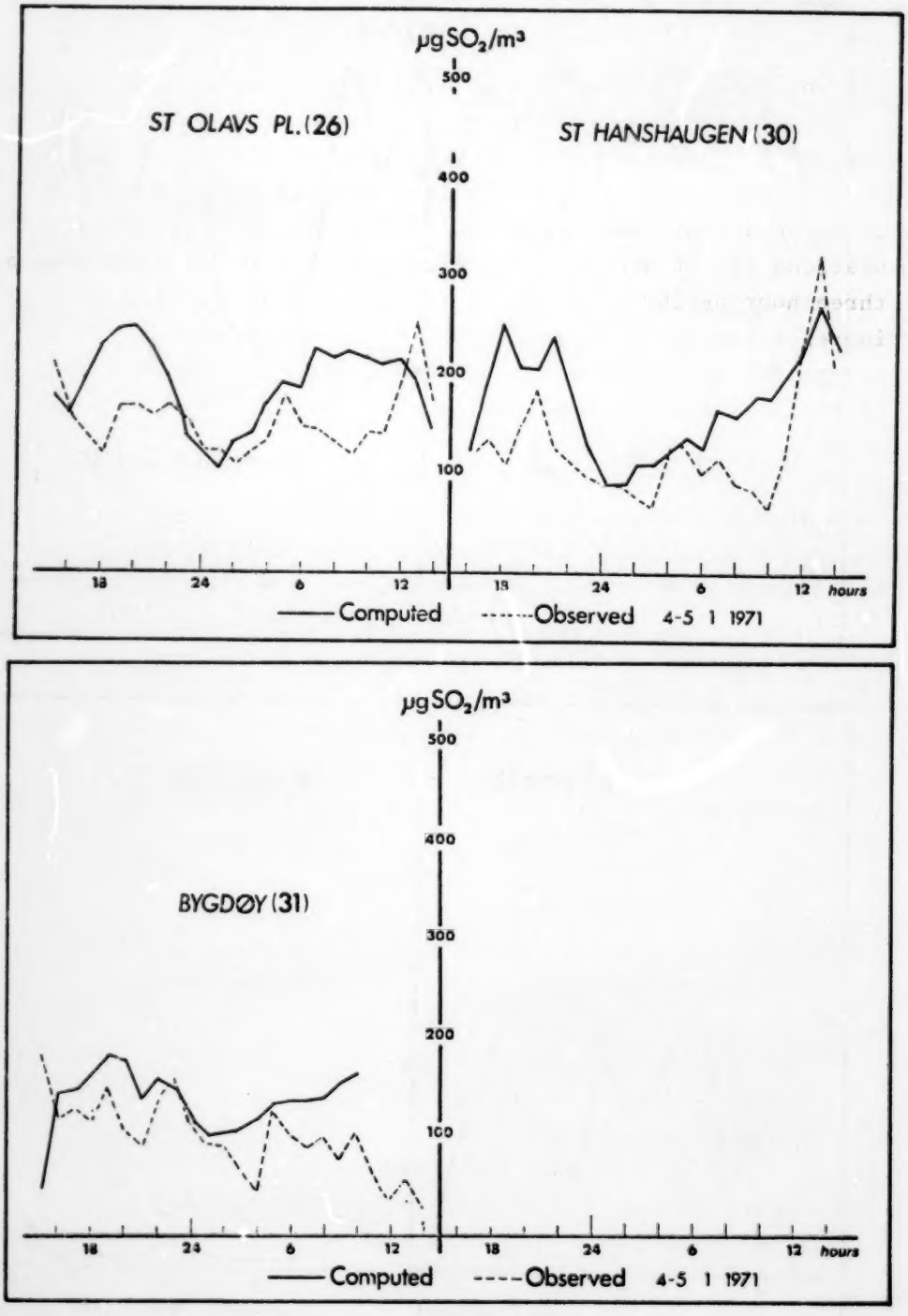

Figure 7.3: Computed and observed SO_2 concentrations.

In Figure 7.2, the calculated and observed concentrations for the 3rd and 4th of January are shown. All over the area, the calculated SO_2 concentrations were somewhat too high. On the other hand, the calculated fluctuations of some hours duration were largely observed in the same manner at the stations 26, 30 and 31. One exception was an increase over a three hour period between 01 and 03h at station 30. This increase was observed somewhat later and with smaller amplitude at station 26. The reason for this might be a local increase of the emission which was not considered in the calculation.

The short term fluctuations in the calculated SO_2 concentrations were mainly due to changes in the wind field. These fluctuations are not easily recognized when the wind field at one of the wind stations is studied. The total ventilation effect resulting from the air flow in several valleys has to be considered. It may therefore be concluded that one wind station is not enough to describe actual short term fluctuations of the air pollution concentration in Oslo. Further, it indicates that small fluctuations in the wind field over the centre of Oslo are fairly well reflected by the network of wind measuring stations (M, N, O and P) placed in the valleys.

Figure 7.3 shows the measured and calculated values for the 4th and 5th of January. The largest discrepancies occurred for the daytime, when the calculated values were much too high.

A similar pattern was found for the 6th of January. These results are shown in Figure 7.4. The calculated and observed values did not match well in the centre of the city. On the other hand, the fluctuations at Bygdøy matched fairly well. The SO_2 concentration at Bygdøy is mainly due to transportation from the centre of Oslo. This means that the transport was fairly well taken into account. The observed values at St. Hanshaugen were remarkably low that day.

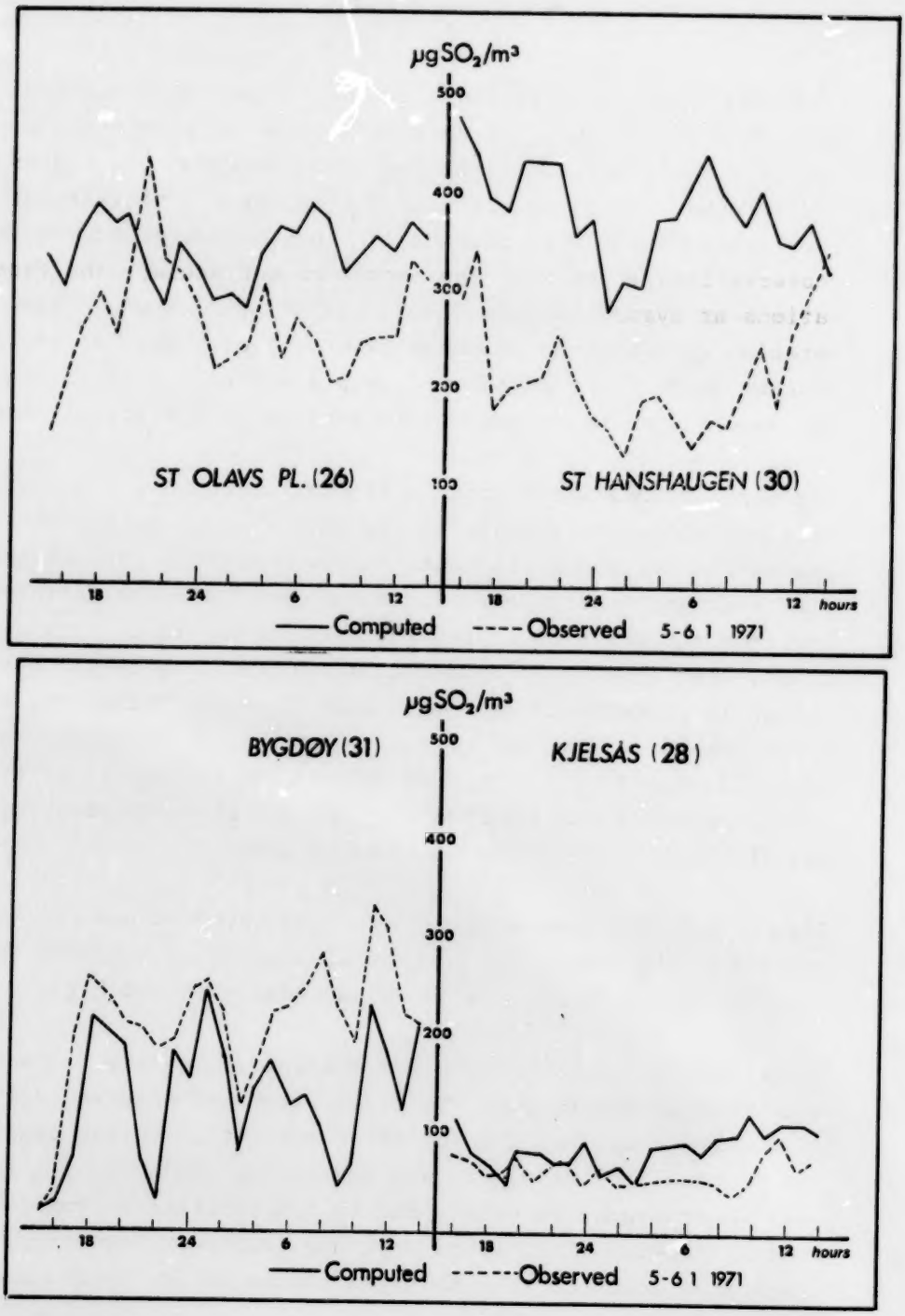

Figure 7.4: Computed and observed SO_2 concentrations.

The correlation coefficient between the calculated and observed hourly SO_2 concentrations from the four stations during the four days were 0.75. This means that much of the variations remain to be explained. On the other hand, many of the calculated short term fluctuations may be recognized in the observations at several stations. In particular, the fluctuations at Bygdøy (Figure 7.4), should be noted when this station is down wind of the centre of Oslo. The resemblance in the short term fluctuations shows that ventilation of SO_2 in Oslo is taken into consideration in a fairly realistic way. The differences between the calculated and observed values have been correlated with other meteorological parameters. The correlation between this difference and temperature and humidity was about 0.80 on all stations. This indicates that more complex chemical processes may have to be considered when trying to improve the model. On the other hand, it is not likely that the SO_2 concentration is sensitive to changes in the chemical processes due to the short residence time in the urban area.

If the applied sink-term for SO_2 is regarded as a source for particulate sulphur, the computed concentrations were of the same order of magnitude as the previously mentioned measurements.

7.4 Concluding remarks

This work is a first attempt to consider systematic vertical motion and inhomogeneous horizontal motion in modeling air pollution near the ground.

In Oslo, the presented wind model (see section 5) worked fairly well in 11 case studies during winter time and gave a reasonable wind estimate also during periods with weak wind conditions that are often observed in Oslo.

Although only about half of the variance in the measured short term SO_2 concentrations is explained, it may be concluded that the ventilation is taken into consideration in an approximately correct way. To show the relative importance of the different removal processes of SO_2 from the ground level in Oslo, the different terms of Equation (7.2) were integrated over the Oslo region, and the results are given in percent of the SO_2 emission:

- removal by vertical transport : 40 - 80%
- " by horizontal transport : 0 - 50%
- " by the applied sink term: 5 - 20%

Due to the organized vertical lifting of the air over Oslo, the SO_2 pollution within the city remains tolerable, despite the high frequency of stagnation periods during the winter.

To study the statistics of the SO_2 concentrations for longer periods of time (3 months) for planing purposes, the model may be integrated over the desired period. This will provide statistics of the SO_2 concentration in different parts of the city as a result of specified emission trends and meteorological conditions.

It should be noted that the vertical diffusion term is left out of the computations, and therefore the calculated concentrations are too high during stagnation periods without inversions. At this stage this effect may be corrected for by a statistical method.

An improvement of the model based on physical considerations may well be possible, but this would demand a multilayer model or anticipations about the boundary layer structure.

8 CONCLUSION

Oslo is a small city compared with other capitals, and the SO_2 emissions are relatively low due to extensive use of electricity. Moderate SO_2 concentrations were observed in the winter periods 1969/70 and 1970/71, and a substantial decrease in the SO_2 pollution was found from the period 1958/63 to the winter periods 1969/70 and 1970/71.

The SO_2 concentrations from the different years have been related to meteorological conditions and the decrease has been estimated to be 30% from 1958/63 to 1969/70 and 30% from the winter 1969/70 to the winter 1970/71.

The vertical temperature stratification was found to characterize the meteorological conditions that are important for the dispersion conditions in Oslo. The dispersion conditions were related to the ambient air concentrations. This relation (model) was used to estimate the reduction in the SO_2 concentrations due to changes in emissions.

This method was also tested against the diurnal emission fluctuations, and the method was found to work well.

The extensive network of wind and temperature measuring stations showed that inversions occur frequently and the mean wind speeds are low. The local wind field and the ventilation conditions are complex.

From a number of case studies during air pollution episodes, some general features of the wind field have been described. An empirical wind model for the Oslo area was developed from two of the case studies and tested against the other 11 case studies.

The model, which works fairly well, was based on continuous wind measurements in the valleys. A model of the three-dimentional wind field along the ground was applied to calculate the short term SO_2 fluctuations from estimates of the emissions in the region. The short term fluctuations were found to be due to the total ventilation effects described by the wind model.

It may be concluded from this wind model study that completely stagnant air will rarely be observed close to the ground in the Oslo basin due to the heat sources located in the lower parts of the area. These induce vertical motions, and therefore the residence time of the air in the Oslo region is in the order of hours and not days.

The present air pollution model for Oslo may be developed further and applied to obtain adequate information for the planning of air pollution abatement, not only for SO_2, but for other pollutants as well, provided an emission survey is available.

Considering the overall air pollution situation in Oslo, the SO_2 pollution does not seem to be the main problem. The pollution of suspended particulates, including its composition of chemical elements, and gaseous pollutants that are emitted from the mobil sources in the area should be investigated to clarify the impacts of these pollutants in Oslo and their future control.

REFERENCES

(1) Lindberg, W — Den alminnelige luftforurensning i Norge. Røykskaderådet (1968).

(2) Nordø, J — On Empirical Deduction of Laws from Geophysical Records. Det Norske Meteorologiske Institutt, Scientific Report No 15 (1966).

(3) Joranger, E; Skogvold, O F; Thyvold, M J; Grønskei, K E — Luftforurensninger i Oslo vinteren 1969/70. NILU Oppdragsrapport nr 15/70. Norwegian Institute for Air Research, Kjeller, 1970.

(4) Reiquam, H — Preliminary Trial of a Box Model in the Oslo Airshed. Proc. of the Second International Clean Air Congress, Washington Dec. 1970. p. 1131.

(5) Bang, J R — Perspektivanalyse for forurensninger. Data for transport. Statens Teknologiske Institutt, Oslo 1972.

(6) Dalaker, O — Om forbrenning av avfall. En oversikt over ovnstyper og forbrenningsmetoder. Teknisk Ukeblad, Bd 119, nr 27, 1972.

(7) Halpern, P; Simon, C and Randall, L — Source Emission and the Vertically Integrated Mass Flux of Sulphur Dioxide Across the New York City Area. Journal of Applied Meteorology, Vol 10, No 4, 1971, p. 715.

(8) Persson, G — Automatic Colimetric Determination of low Concentrations of Sulphate for Measuring Sulphur Dioxide in Ambient Air. Air and Water Poll. Int. J. 10 (1966) p. 845.

(9) Anda, O — An Automated Method for Quantitative Determination of Sulphur Dioxide (SO_2) Concentration in Air (The Thorin Method) Norwegian Institute for Air Research, Kjeller TN 48/73 (1973).

(10) — Organisation for Economic Co-operation and Development(OECD). Methods of measuring Air Pollution. Report of the Working Party on Methods of Measuring Air Pollution and Survey Techniques. Paris 1964.

(11) — Statens Luftvårdsnämd (Sweden). Rekommendationer rörande riktvärden för svaveldioxidhalten i utomhusluft. Meddelande 6601, 1967.

(12) — Environmental Protection Agency (EPA), USA. EPA Proposes National Air Quality Standards. Journal of the Air Pollution Control Association (APCA) Vol 21, No 3 (March 1971). p. 149.

(13) Bringfelt, B — Important Factors for the Sulphur Dioxide Concentration in Central Stockholm. Atmospheric Environment 1971 Vol 5. No 11, p. 949.

(14) US Department of Health, Education and Welfare. Air Quality Data from the National Air Sampling Networks and Contributing State and Local Networks. 1966 Edition.

(15) Brun, J — Standard Normals 1931-60 of the Air Temperature in Norway. Det Norske Meteorologiske Institutt (Norway) Oslo 1967.

(16) Johannessen, T W — Monthly Frequencies of concurrent Wind Forces and Wind Directions in Norway. Det Norske Meteorologiske Institutt (Norway) Oslo 1960.

(17) Peterson, J T — The Climate of Cities, A Survey of recent Literature. US Department of Health, Education and Welfare, Oct. 1969.

(18) Wanta, R C — Mathematical Models of Urban Air Pollution. Air Pollution, Vol 1, p. 215, edited by A C Stern, Academic Press, New York, London 1968.

(19) Neiburger, M — Diffusion Models of Urban Air Pollution Technical Note No 108, World Meteorological Organisation, WMO, No 254, TP 141, p. 248.

(20) Kohn, R E — Abatement Strategy and Air Quality Standards. Development of Air Quality Standards. Edited by Arthur A Eriksen and Richard S Gaines.

(21) Grønskei, K E — A Time Dependent Numerical Dispersion Model for Air Pollution with Apllication to the City of Oslo. Norwegian Institute for Air Research, Kjeller IR 20/71 (1971).

(22) Norwegian Institute for Air Research.
The OECD-project. Cooperative Technical Programme to Measure the Long Range Transport of Air Pollutants. Development of the Project and Preliminary Results.
Kjeller, January 1973. P. 23.

*U.S. GOVERNMENT PRINTING OFFICE:1973 514-153/235 1-3